SISSA - SCUOLA
INTERNAZIONALE
SUPERIORE
DI STUDI AVANZATI
TRIESTE
Strada Costiera 11

ISAS - INTERNATIONAL SCHOOL FOR ADVANCED STUDIES

THESIS SUBMITTED FOR THE DEGREE

OF

"MAGISTER PHILOSOPHIAE"

LONG TERM VARIABILITY IN THE SPECTRUM OF GAMMA CAS. THE HEI LINES

Candidate:

Antonella Porri

Supervisors:

Prof. R. Stalio
Prof. G. Sedmak

Academic Year: 1984/85

TRIESTE

INTRODUCTION

Since more than a decade, space observations have shown the ubiquity of stellar winds and heated atmospheric regions in all classes of stars across the HR diagram. They have strongly modified our outlook on stellar atmosperes, that once were thought to be in radiative equilibrium, hydrostatic equilibrium and not exchanging mass with the enviroment.

Combined space and ground observations have shown that the existence of circumstellar envelopes is likely associated whith variable mass loss. In particular variable mass loss can be associated with the existence of the Be phenomenon and of Be star variability.

All present theories are inadequate for explaining the mechanisms which produce the heated regions in the atmospheres of early type stars, and the origin of mass loss and its variability.

Thus it is necessary to find an explanation of the origin of this phenomena which is consistent with (1) the fact that, among early type stars of the same spectral type and luminosity class, there are some with detectable mass loss and some where mass loss is not observed, (2) consistent with the existence of heated regions, and with (3) the observed variability.

Recently it has been suggested (Stalio and Zirker, 1985) that radial and non-radial pulsations might play an important

role in exploring points (1) through (3) above.

This work is part of a larger program that has the aim to explore what is the role of photospheric motions in the exo-photospheric structure and dynamics of B stars.
The observational side of this program includes simultaneous observations in the visible and UV spectral regions of a selected sample of normal B and Be stars. We plan to observe, from ground telescope, at high resolution and with high signal to noise ratio, HeI and/or SiIII line profiles in order to measure profile shape variability and infer, from their amplitudes and time scales, on photospheric motions. We will also look for, from space telescopes, for variability of UV continuum distribution and of UV lines, which indicate mass loss and heated atmospheric regions.

We specifically aim at
(a) to establish what is the range of the UV variability;
(b) to determine what is the relation of this variability with mass loss and with chromospheric/coronal regions;
(c) to determine what is the relation of this variability with the dynamics of the photosphere.

In the context of this general program, we study in this thesis HeI line profile variability in a Be star, Gamma Cas. The data set on which this work is based consist of 46 spectra obtained in the years 1972-1981 at the Haute-Provence Observatory.
We want to infer on the photospheric motions and relate them to the outer atmosphere characteristic which have been studied by

Doazan et al.(1983) using the same data set.

It is worthwhile to recall that Be stars are, among the main sequence B stars, those with larger amplitude of mass loss and variability of it. Recently evidences have been accumulated for the existence of rapid variations in the absorption lines of Be stars which have been linked to the axistence of one or several radial oscillation modes (see Stalio and Zirker, 1985).

Rapid variations of the photospheric lines have not been detected in our data set. The reason is that, despite the excellent quality of our spectroscopic material, the noise level of photographic observation makes difficult to detect asymmetries or "bumbs" similar to those which are detected in other pulsating stars when the observations are made with modern detectors.

However, even if there are not evidences for short period variations, interesting results have been obtained from the analysis of line profile variations that occur on longer time scales.

In the following section (I) the basic properties and classification of non-radial oscillations are given and the observational aspects of radial and non-radial oscillations are summarized. In section II the characteristic properties of the Be stars and in particular of the star under study, Gamma Cas, are described. In section III we explain the data processing method. In section IV we present the observational results. In section V we discuss the results.

I STELLAR PULSATIONS

I.1 Historical Background and Recent Development

Pulsating stars are stars in which large-scale, periodic or quasi-periodic motions, usually including the entire star, are present. The simplest kind of such motions is a purely radial pulsation: the star maintains a spherical shape at all times, but changes its volume. In a non-radial pulsation the stellar form periodically deviates from the spherical shape.
Pulsating stars comprise only a subset of the wider class of "intrinsic variable stars", that is stars whose variability arises from causes entirely within themselves, and not from geometric effects such as eclipses in binary stars.

The variations associated with the pulsating variables may be periodic or cyclic, semi-regular or irregular. The corresponding time scales range from a few seconds to a few years (Cox, 1980).

The idea that certain types of variables stars owe their variability to periodic or cyclic expansions dates from the work of Shapley (1914), and was given a firm mathematical fondation in 1918 by Eddington (the early history of studies on stellar pulsation was described by Rosseland in Chapter 1 of his book "The Pulsation Theory of Variable Stars", 1949) Since then the study of pulsating stars has proved a powerful tool in the study

of stellar structure and in other branches of astrophysics. One of the important results of the observational study of one of the best-known types of pulsating stars, the Classical Cepheids, is the famous period-luminosity relation that has played a crucial role in the establishment of the basic distance scale of the Universe.

The present thesis is restricted mainly to discussion of non-radial oscillations in early type stars. We want to verify, observationally, if there exist some support to the recently claimed relationship between existence of non-radial pulsations and mass loss in early type stars. It has been so for a quite remarkable progress in both observational and theoretical studies of non-radial pulsations in different kinds of objects. The theoretical study of non-radial stellar pulsations receveid a great boost with the publication of the Handbuch articles by Ledoux and Waldraven (1958); but the advent of quantitative computing did not occur until the work of Dziembowski (1971) and Osaki (1971).

The development of the study of non-radial pulsation may be regarded to have started from the recognition of double periodicity in the light curves of Beta Cephei stars. These light curve can be decomposed in two periods. Similar variations are observed in the line widths of Beta Cephei stars. Since it seemed unlikely that purely radial oscillations are responsible for these phenomena, Ledoux (1951) proposed that these stars undergo non-radial oscillations in the presence of rotation.

Osaky (1971) compared the stars to musical instruments which have various modes of oscillation and tones. As we will show later, the normal modes, in a spherically symmetric star, are characterized by the eigenfunctions that are proportional to the spherical harmonics: $Y_l^m(\theta,\phi)$ ($l=0,1,2,\ldots;m=\pm1,\pm2,\ldots,\pm l$). The eigenfrequencies depend on l but are degenerate by (2l+1) folds in m. The degeneracy in m arises from the symmetry of the equilibrium structure around an arbitrary axis. If a slow rotation or a weak magnetic field is introduced, the degeneracy is resolved. In the case of radial pulsations it is difficult that two oscillations with nearly equal periods occur. But in the case of non-radial oscillations nearly equal periods can be explained in terms of the rotational splitting of eigenfrequencies with the same l but differing m.

Another impetus to the study of non-radial oscillations came from the discovery of the solar five-minute oscillations by Leighton, Noyes and Simon (1962) and the interpretation of this in terms of non-radial oscillations of the Sun.

From 1970, when the pulsation of Beta Cephei stars and the solar five-minute oscillation were the only cases in which non-radial pulsations were suspected as a possible cause, the situation has changed drastically.

1) Observations by Mc Graw and coworkers (1977) suggested the existence of a new class of non-radial pulsating stars, the "ZZ Ceti" stars. These stars were thought to be ordinary white dwarfs. They are characterized by a very short-period light variations (the period ranges from about 20 sec. to about 1000

sec.) that are for the most part quite irregular.

2) Lucy (1976) detected multiple periodicity and beat phenomena in an early supergiant, Alpha Cygni.

3) Smith (1977) found many upper near main-sequence stars with variable line profiles similar to the Beta Cephei type. These stars are sharp lined O8 to B5 near the main-sequence, surrounding the Beta Cephei domain without being included in it. Smith concluded that their line profile variations can only be understood as resulting from non-radial oscillations. He has called these stars "line profile variable B stars", or "53 Persei stars".

Recent observational development has been very rapid. Quasi emission absorption "bumbs", traveling blu-to-red across the line profiles of Zeta Oph and Spica (see Figure 1), have been detected by Walker et al. (1979, 1981). Vogt and Penrod (1983) demonstrated that non-radial pulsation modes are responsible for these features in Zeta Oph. Line profile variations have been detected in Eps. Per (Smith, 1984) and in Eta Lep.

Smith and Penrod (1985) observing twenty Bn (these are among the B stars that with higher measured rotational velocity) or Be stars, found convincing evidence for non-radial pulsation in 13 of them (one star is a rapidly rotating Beta Cephei star), and probable profile variations in all the others. Several of their stars also show photometric evidence for non-radial pulsation. Baade (1984) found two non-radial pulsation modes in a Be star, Mu Cen (B2Ve).

Now it seems time to state that there is not a real

distinction between sharp line stars like the "53 Persei" stars and this rapid rotating, non-radial pulsators and that non-radial pulsations can be present at all rotational velocities, probably in all late-O/early-B stars.

Near the main sequence, non radial pulsation probably continues to about B6 on the cool side and to O6 in the hot side (Smith and Penrod, 1985). Several investigators (Burki et al., 1978, Maeder and Rufener, 1981, Smith and Ebbets, 1981) have suggested that O-B supergiants exhibit optical wavelength short-timescale light and/or line profile variations.

Developments in high-precision and high-speed spectroscopic observations will open a new era for the observations of stellar variability in the future.

A number of theoretical problems still remain to be studied in more detail. Among them are:

a) oscillations in the presence of a strong magnetc field or rotation;

b) energy and momentum transfer by waves to the outer atmosphere of the pulsating star;

c) link between mass loss and pulsation..br; In additon the specific driving mechanism of the stellar pulsation theory remains to be fully understood.

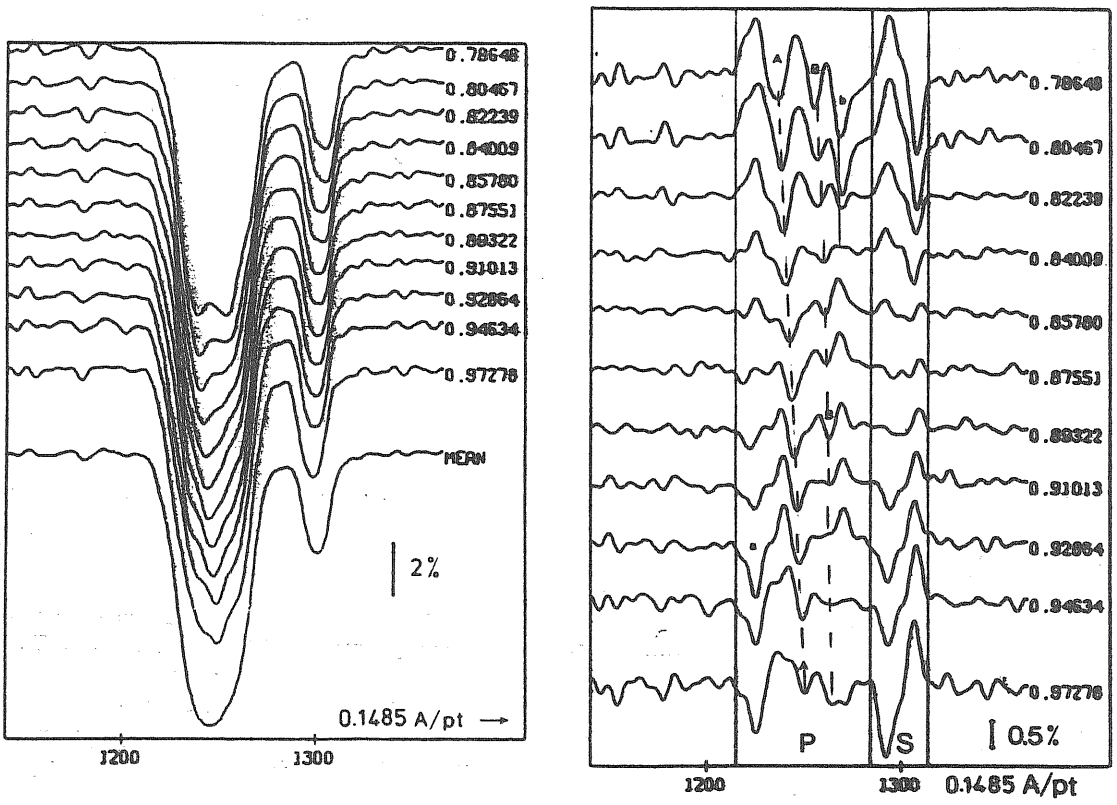

Fig.1. The 1981 April 14 HeI 6678 line profiles of Spica and residual from the mean profile. Three moving features A,B and b are identified (from Walker et al., 1979-1981).

I.2 Basic Properties and Classification of Non-Radial Pulsations

In this section we explain the basic properties of non-radial pulsations, and introduce the related formalism. Development of the detailed equations for the non-radial pulsations have been given in two books. These are by Unno, Osaki, Ando and Shibahashi (1979) and by Cox (1980).

The simplest theoretical treatment of non-radial pulsations is under the assumption of the linear and adiabatic approximations. The system of equations, which describes the linear adiabatic non-radial oscillations, forms a boundary-value problem of fourth-order ordinary differential equations in the radial coordinate r, and for a given stellar equilibrium model, eigenvalues and eigenfunctions are to be calculated numerically.

The assumption ,for solving this system of equations, is that the motions can be separated into a function of the radius alone times a tangential term which is a spherical harmonic, consisting of the associate Legendre polynomial and a m-fold longitudinal sinusoidal variation. So the perturbations of the physical variables take the following form:

$$p\,(t,r,\theta,\phi) = P'(r)Y_{\ell}^{m}(\theta,\phi)e^{-i\sigma t},$$

where P is the Eulerian pressure perturbation. And the corresponding expression for the displacement vector (=r-r), where r is the radial distance and the subscript o denotes the imperturbed state) is given by

$$\underset{\sim}{\xi}_{\ell} = [\xi_r(r), \xi_h(r)\frac{\partial}{\partial\theta}, \xi_h(r)\frac{1}{\sin\theta}\frac{\partial}{\partial\phi}]Y^m_\ell(\theta,\phi)\ e^{-i\sigma t},$$

where

$$Y^\ell_m(\theta,\phi) = P^m_\ell(\cos\theta)\ e^{im\phi},$$

$P^m_\ell(x)$ denotes the associated Legendre polinomial, k indicates the number of nodes $\xi^\ell_{r,k}(r_i)=0$ $(i=1,2,\ldots,k)$ execept r=0, $l(=0,1,2,\ldots)$ and $m(=-l,-l+1,..,0,\ldots,l-1,l)$ are integers. The quantity σ is the eigenfrequency of the non-radial oscillation which is specified by three integers (k,l,m).

The quantum number l represents the number of border lines (lines of zero motion) by which the stellar surface is divided to oscillate in the opposite phase.The radial modes correspond to the special cases of l=0. The other Harmonics are called the dipole (l=1), the quadrupole (l=2), the octapole (l=3) oscillations, etc.. For a given l, the number m takes integer values from -l to +l, and the eigenfrequencies of these (2l+1) modes are degenerate in a spherically symmetric (non-rotating, non magnetic) star.

We can adequately study the adiabatic oscillations to a first approximation, by neglecting non-adiabatic effects and viscosity. It is obvious that, since the oscillations are assumed to be adiabatic (no net heat gains or losses by the oscillating mass elements), this case can not tell us how the luminosity of a pulsating star changes during the pulsation. It is clear, moreover, that this theory cannot yield information regarding the "pulsational stability" of a star. Oscillations assumed to be present initially will maintain the same amplitude

for all time. In the case of nonadiabatic radial oscillations, since the system is no longer conservative, we can expect to find solutions with complex frequencies. In this case the solutions are characterized by secularly increasing or decreasing pulsation amplitudes. Nevertheless the simple adiabatic theory gives, in most cases, a good description of many features, such as the periods of the pulsating stars, and the relative pulsation amplitude within the star. The main reason of these facts is that in stars the dynamical time scale is much shorter than the thermal time scale (by a factor 10 for the Sun).

The richness of non-radial pulsation compared with radial pulsation is only due to the degree of freedom in the horizontal wave number represented by the quantum number l. Besides that two different kinds of restoring force, the pressure force and the buoyancy force, operate in non-radial pulsations. Since the change in gravitational force is inward in the compressed phase, or outward in the expanded phase, gravity cannot be the restoring force for the radial pulsation. On the other hand gravity can act through buoyancy as the restoring force for non-radial oscillations. So two different kinds of modes exist in non-radial oscillations: pressure (acustic) modes and gravity modes. The pressure modes (p-modes) form a sequence of increasing eigenfrequency with the order of the modes specified by the number of nodes, i.e.,

$$\sigma_{p_1} < \sigma_{p_2} < \sigma_{p_3} < \ldots\ldots \to \infty \quad .$$

The gravity modes (g-modes) form a sequence of decreasing frequency, i.e.,

$$\sigma g_1 > \sigma g_2 > \sigma g_3 > \ldots\ldots \to \infty \quad .$$

There are two characteristic frequencies governing the oscillatory property of the medium. One of them is the Lamb frequency, L_ℓ, given by

$$L_\ell^2 = \frac{\ell(\ell+1)}{r^2} c^2 \quad ,$$

where c denotes the speed of sound. The other characteristic frequency is the Brunt-Vaisala frequency denotated by N

$$N^2 = g \left(\frac{1}{\Gamma_1} \frac{d \ln p_0}{dr} - \frac{d \ln \rho_0}{dr} \right) \quad ,$$

where g is the gravitational acceleration ($=GM_r/r^2$), p_0 and ρ_0 the pressure and the density of the imperturbed state, and Γ_1 the adiabatic exponent ($= d \ln p / d \ln \rho$). A sound wave travels a wavelength $2\pi r/l$ horizontally in the period $2\pi/L_\ell$ and a blob of gas oscillates vertically, with positive or negative buoyancy under the local pressure balance with frequency N.

For high frequencies ($\sigma^2 > L_\ell^2, N^2$), the relative Eulerian pressure perturbation, p'/p_0, dominates the relative radial displacement ξ_r/H, where H denotes the pressure scale of height ($H=p_0/\rho_0 g$). These large Eulerian pressure variations are responsible for most of the restoring forces which act during the oscillations. For low frequencies ($\sigma^2 < L_\ell^2, N^2$), p'/p_0 is less then ξ_r/H the restoring force is due to the force of gravity. In the other regions ($L_\ell^2 > \sigma^2 > N^2$ or $L_\ell^2 < \sigma^2 < N^2$), the

eigenfunction does not show spatial oscillation but decreases exponentially with the distance from the wave propagation; these are called evanescent regions. The region in which both $\sigma > L_\ell$ and $\sigma > N$ is called the p-wave propagation zone, and the region in which both $\sigma < L_\ell$ and $\sigma < N$ is called the g wave propagation zone. The energy of oscillation is mainly trapped in the propagation zone. The two propagation regions, separated by the so called evanescent zone, are coupled with a sort of "tunnel effect".

Figure 2 shows the propagation diagram given essentially by Sculfaire (1974) for a polytrope (index 3) model. This diagram shows in what part of the stellar interior a wave with a given frequency has locally a propagating or non-propagating character. Generally, non-radial p-modes are oscillations trapped near the surface and g-modes are those trapped in the deep interior.

The propagation diagram may be comparable to the potential energy function of the one-dimensional Schrödinger equation of quantum mechanics in such a way that a propagation zone correspond to a potential well and an evanescent zone to a potential wall. Since eigenmodes are standing waves, they occur in a region of a potential well, that is enclosed by potential walls at both ends. The most important difference lies in the fact that in the case of non-radial oscillations there are two different kinds of potential wells: one is that opened upward (p-wave zone) and the other is that opened downward (g-wave zone).

Since we are interested in those oscillations that may produce observable motions in the stellar atmosphere, the most important modes are those of non-radial p-mode oscillations. Furthermore oscillations of nonradial p-modes are more strongly concentred near the surface as the spherical harmonics index l is increased. This can be seen in the propagation diagram, because the Lamb frequency, L_l, moves upward with increase of l. The classification of modes, however, is not so simple in reality as outlined above. If a convective zone ($N^2 < 0$) exists within a star, the spectra of unstable modes appear. The convective modes are often designed by the g⁻- modes. For the g⁻-modes, $\sigma^2 < 0$ and $|\sigma^2|$ decreases as k increases. Therefore complication arises when $N^2(r)$ changes in a complicated way, especially because of the evolutionary inhomogeneity in the mean molecular weight distribution.

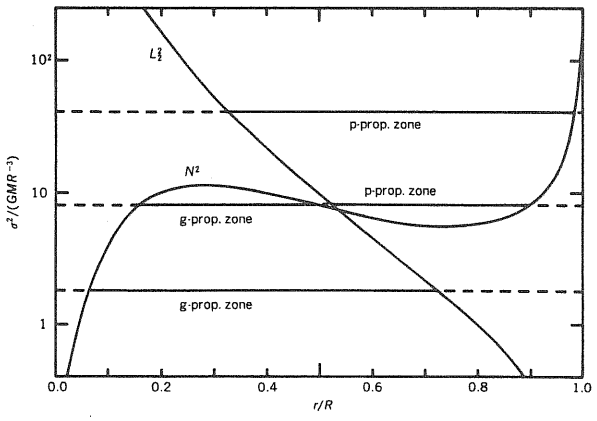

Fig.2. Variations of N^2 and L_l^2 (l=2 normalized by GM/R^3 where M and R are the mass and the radius of the star) for a polytrope (index n=3) model. Three horizontal lines show the wave propagation zones

I.3 General Remarks on Observational Aspect of Radial and Nonradial Oscillations

We now consider the observational side. We have summarized in Table 1 some of the properties of most recognized types of pulsating variables and various observational phenomena for which non-radial oscillations have been suggested. In Figure 3 are shown the locations in the HR diagram of some of these stars.

It is now well established that variable stars such as Cepheids, RR Lyrae, and Mira variables are pulsating stars and their pulsations are explained in terms of simple radial, spherically symmetric pulsations. The light curves of these variables are symmetric and highly periodic. The radial velocity curves tend to be roughly mirror images of the light curves, when the astronomical sign convenction regarding radial velocities is used, as shown in Figure 4. If the velocity curve represents the motion of stellar surface, then the phase relation between the light and velocity curves implies that the star is brightest when it is expanding and not when its radius is smallest, as might be expected on the basis of a naive application of adiabatic pulsation theory.

Now we will discuss how non-radial oscillations manifest observationally and how they can be distinguished from radial pulsations.

In the case of radial pulsations, the period of the fundamental mode is longer than those of the higher harmonics. In the case

of non-radial oscillations, the p-modes have periods similar to those of corresponding radial modes, but in general g-modes have periods much longer than those of radial pulsations. If a group of pulsating stars has period much longer than that expected theoretically for the radial fundamental mode, it is possible that pulsations of these variables may be explained in terms of non-radial g-modes (white dwarfs variables are a good example of this case).

In some variable stars the light curve and/or the radial velocity curve are not periodic but can be decomposed in more periodic variations per star. This is the so-called beat phenomenon; the simple explanation for it may be the simultaneous excitation of more oscillations with nearly equal periods. As we have already said, in the case of radial pulsations it is difficult for two oscillations with nearly equal periods to occur. But in the case of non-radial oscillations, the existence of nearly equal periods can be easily explained in terms of rotational splitting of eigenfrequencies of non-radial modes with the same quantum numbers k and l but differing in m.

The beat phenomenon has been used to infer non-radial oscillations for the Beta Cephei stars and white dwarfs variables.

In non-radial oscillations different parts of the surface of a star move in different ways, and this kind of motion must affect spectral line profile.

Line profiles in stars undergoing non-radial oscillations were

calculated and compared with observations by Osaki (1971), Smith (1977) and Kubiak (1978).

Osaki (1971) preferred, for both theoretical and observational reasons, the l=2 m=2 non-radial mode for simulate the characteristic line profile variations observed in some of the Beta Cephei stars. And this non-radial mode explained successfully the line profile variations discovered by Smith (1977) in the "53 Persei stars".

The dipole oscillations (l=1) and the octapole oscillations (l=3) may also yield variations similar to those of l=2 (Kubiak, 1978). On the other hand, the higher harmonic deformations (l > 4) may be less likely to cause large variations in line broadening because they tend to cancel themselves over the disk of the star.

There exist five distinct modes m=-2,-1,0,+1 and +2 belonging to the quadrupole mode (l=2), and their eigenfrequencies are degenerate in the case of no-rotation.

Let us see the reasons for prefer the l=2, m=2 mode for simulate the line profile variations of non-radial pulsating stars.

The phase velocity of waves traveling around the rotation axis is given by

$$(d\phi / dt)_{phase} = \sigma / m \quad .$$

Thus, modes with positive and negative m represent traveling waves in the same and the opposite directions with respect to the rotation, while mode with m=0 represents a standing oscillation symmetrical to the axis of rotation.

This last mode can be excluded because it produces only small changes in the profiles. The modes with m<0 produce line profile variations in the "wrong" sense with time, that is they don' t fit the observed variations. The l=2, m=1 mode is acceptable but it is less favoured theoretically.
In Figure 5 the spherical harmonics motions are shown for l=2 and m=2. In the same figure we give the equatorial velocities in this case as a function of the longitude. One can see that the various parts of the star have different radial velocities, and the Doppler shift for each small area of the surface varies over the surface.

Line profile for a rotating star undergoing non-radial oscillations can be calculated by a method described by Osaki (1971). We choose a mode which is specified by integers l and m, and the inclination, i, of the axis of rotation relative to the line of sight. We then divide the star' s visible disk into many surface elements, and calculate the velocity of each element due to the combined effect of rotation and nonradial oscillation. The velocity of a mass element over the surface of a star undergoing non radial oscillations can be written in spherical coordinate

$$V_{osc} = A\left(1+K\frac{\partial}{\partial\theta}, K\frac{1}{\sin\theta}\frac{\partial}{\partial\phi}\right)P_l^m(\cos\theta)e^{im\phi},$$

where A and AK stand for the amplitudes in the radial direction and in the horizontal direction, respectively. The line profile is then formed by adding up the intensity from each element with due accounts of a Doppler shift corresponding to the line of

sight velocity and of a weight appropriate to the limb darkening law. In Osaki' s calculations, variations in surface area and brightness due to the oscillation and effect of intrinsic broadening of lines, such as thermal Doppler and microturbolence broadenings, were neglected. In such a case, if the basic parameters such as the limb-darkening coefficient, the inlination, i, the pulsation mode (l,m) and the ratio of the horizontal to the radial velocity amplitudes, K , are fixed, there remains only one free parameter which correspond to the amplitude of pulsation, A.

For a wave traveling in the same direction as the rotation, l=2 and m=2, the line profiles are shown in Figure 6 for A/Ve=.4, where Ve is the equatorial rotational velocity, K =.15, and i=90 . As seen in Figure 6, the variation in line profile looks as if a kind of wave were sweeping over the rotationally broadened profile once per cycle. A weak component first appearing on the violet edge of the profile, moves towards the center increasing in intensity; and then towards the red edge decreasing in intensity and increasing in half-width. The line takes a dish-shaped profile at Φ =.75. When the red component disappears, a new violet component appears and a new cycle is then repeated. These characteristics simulate very well the observations of Beta Cephei stars with variable line broadening and the line profile variations discovered by Smith (1977) in the "53 Persei stars".

Non-radial oscillations with higher spherical harmonics may not give rise to light variation or line profiles variations,

but they may manifest themselves as surface velocity fields. It may then happen that certain kinds of dynamical phenomena, such as macro- and micro-turbolence, or the heating of stellar corona could be caused by these non-radial oscillations also.
However more theoretical and observational studies are needed to reveal this subject.

TABLE 1

Kind of Star	Phenomena	Evidence for NRO	Period	Spectral Types	Absolute Magnitude	References
RR Lyrae	Periodic light and radial velocity variations		15-24 h	A2- F2	0 / 1	See Cox & 1980
Classical Cepheids	"		1-50 d	F6- K2	.5 / -2	"
β Cephei Stars	Pulsating variables	Beat and line profile variation	4- 6 h	B1- B2	-3.5/-4.5	Ledoux 1951 Osaki 1971
δ Scuti Stars	"	Multiple Periodicity	1- 3 h	A2- F5	2 / 3	Dziembowski 1971
ZZ Ceti Stars	Periodic light variation	Length of periods	10-10 s	A5- F5	10 / 15?	Mc Graw & Robinson 1976
Early Type Stars	Line prof. variation	Line profile variation	1- 2 h	O8- B5	- 3 /- 5	Smith 1977
Late Type Giants and Supergiants	Chromosphere	Heating of upper atmosphere	10-200d	M,N,R,S	-1 /- 3	Ando 1976
Early Type supergiants (α Cygni)	Semiregular radial velocity variations	Multiple periodicity line width	10-100d	A1- G0	- 3 /- 5	Lucy 1976
The Sun	5 min. oscillatio		5 m	G2	4.83	Ando and Osaki 1975
The Sun	Global oscillation	Length of periods				Christensen Dalsgaard Gough 1976

* The very existence of global oscillations of the sun is still a matter of contrversy among observes

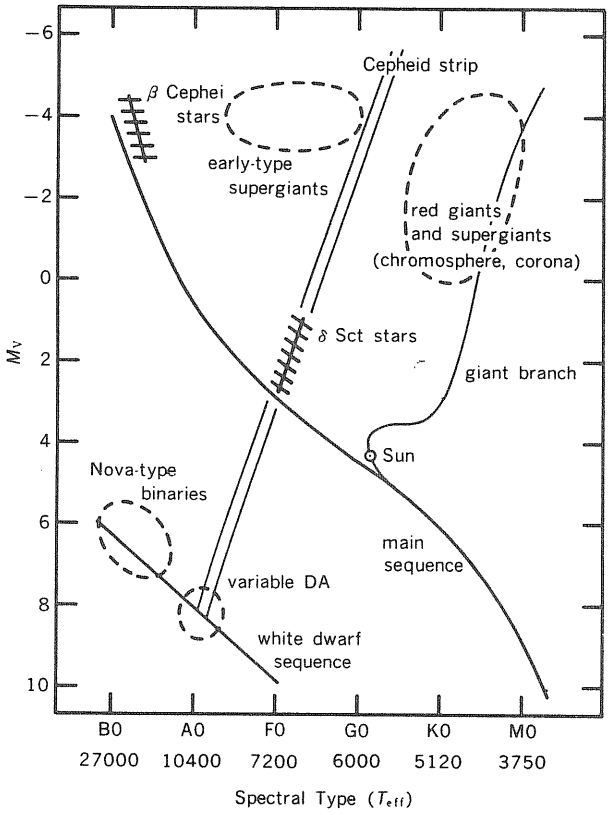

Fig.3. Location of a number of various types of pulsating variables on the HR diagram (from Unno et al.,1979).

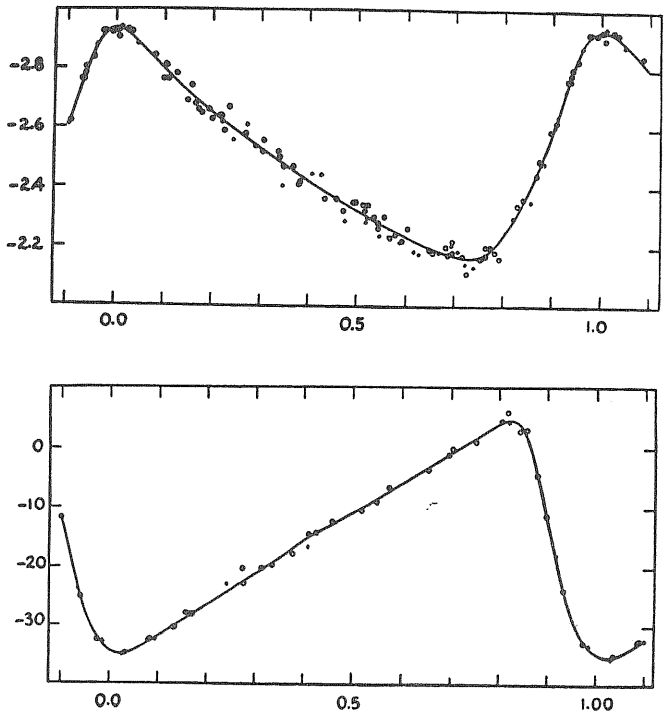

Fig.4. Light curve (upper) and radial velocity curve (lower) for Delta Cep (from Cox, 1974).

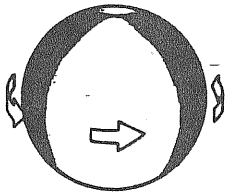

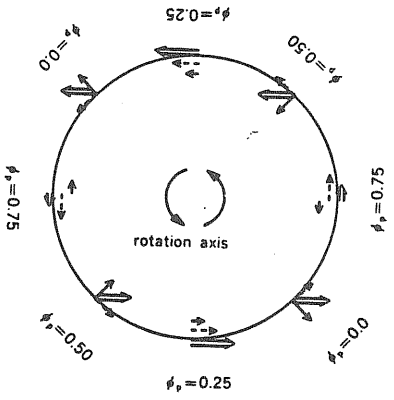

Fig.5. a) The spherical harmonic motions are shown for l=2 and m=2. b) Equatorial velocities in this case as a function of the longitude. The rotation velocity is given by the dashed arrow, the pulsation velocity by the solid arrow, and the big arrows show their vector addition at eight points around the equator.

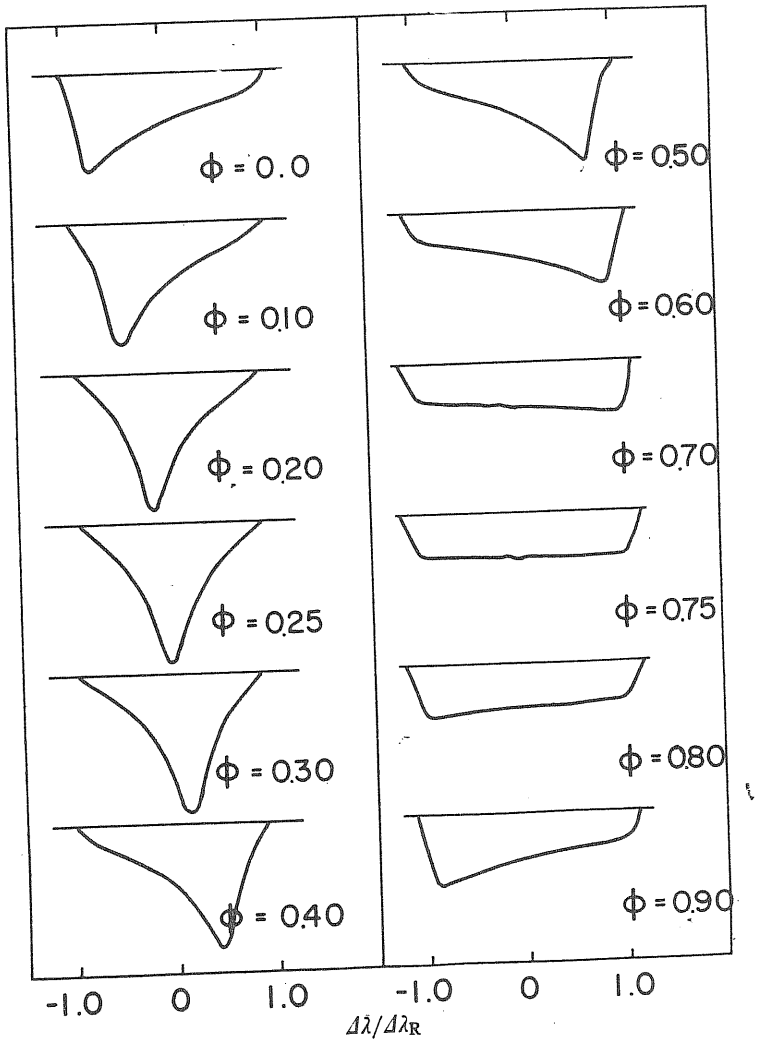

Fig.6. Variation of the line profile with phase for A/V =.4 K=.15 and i=90 . The abscissa is $\Delta\lambda/\Delta\lambda_R$ and the ordinate uses an arbitrary scale (from Osaki, 1971).

:

II THE STAR UNDER STUDY :
GAMMA CAS (B 0.5 IVe)

II.1 Introduction to Be Stars

Among main sequence and giant B stars a large fraction (~20%) exhibit hydrogen emission lines in the visible wavelength range. These lines are often accompanied by emission lines of singly ionized metals. The presence of emission lines is an anomaly in the system used to classify stellar spectra at visible wavelengths and also in the classical theory of stellar atmospheres, which predicts only absorption lines.

Struve (1931) attributed the origin of the emission lines in the visible spectra of Be stars to an extended envelope, confined to the equatorial region, where the gas is ionized by the ultraviolet radiation of the star; thus the emission spectrum is a recombination spectrum. The existence of an extended atmosphere was attributed by Struve to the ejection of matter from these stars at the equator, due to rotational instability. Thus, according to Struve's model, the Be phenomenon is limited to stars which rotate at critical

velocity. Presently, Struve's model and more recent models based on his idea encounter serious difficulties in explain the spectral variability of Be stars. Infact Be star can lose and recover all of their emission features in the course of time. Transitions from a Be spectrum (H emission lines with a more or less central reversal) to a shell spectrum (H absorption lines with very narrow and deep cores which may or may not be bordered by emission wings), and to a normal B spectrum may be made in any direction.

Also in the high energy part of the spectrum (X-rays and far-UV) Struve like models fail because they don' t explain the presence of higly ionized regions, with temperature of the order of 10^5 °K, mass flow velocity exceeding the stellar escape velocity of the star surface both for pole-on stars and equator-on stars, variability of this mass flow.

Presently everybody agree that Be-star models must be rethought on an observational basis which covers the broadest wavelength range possible, from the X-ray and far-UV to IR and radio regions, it is necessary to account for the observed high velocity, superionized regions and simultaneously for the low-velocity, cool, extended H-alpha emitting envelope; and for the variabilyty of this structure.

Besides the "phase" variations (Be, Be-shell, B-normal) and the mass loss variations (from FUV spectrum), rapid variations, which are probably due to non-radial pulsations, have been discovered.

In 28 CMa, Baade (1982) found changes in the asymmetry of the

lines as a whole, similar to those observed in the Beta Cephei stars.Smith and Penrod (1985) found convincing evidence for non radial pulsations in many stars of a sample of observed Be stars.

Further evidence have been now accumulated for the existence of rapid variations in the absorption lines of Be stars spectra even if the small amplitude of these variations makes them difficult to detect.

II.2 General Characteristics of Gamma Cas

In this section we present the long term variations of Gamma Cas in the visual until 1981. We essentially describe the spectral behaviour which give us information on the cool H-alpha emitting region of the outer atmosphere. Also we present a short comparison of these visual data with the basic assumptions and predictions of current models.

Secchi (1866) discovered the first Be star by observing the H-beta line in emission in the spectrum of Gamma Cas. Since then Gamma Cas been very intensively observed in many different features of its spectrum. Its visual spectrum has exhibited in turn a long Be phase, from 1866 to 1932, followed by complex phase changes, from 1932 to 1942, at the end of which the star has falt back into a quasi normal B phase. During this episode two, strong and brief, shell phases, following two very intense

emission phases, were observed; from 1942 to 1981, the star went from a quasi normal B phase to a second, slowly and irregularly increasing Be phase.

The majority of the Be stars have been observed in a single phase, Be or shell, much less frequently than Gamma Cas, and over a much shorter time span. If the Gamma Cas behaviour is typical, this shows that the description of the Be phenomenon requires the analysis of observations made on time scales of the order of a century, rather than a few decades (Doazan, 1982).

The spectrum of Gamma Cas and its long term variations have been fully described by Edwards (1956), Kitchin (1970), Cowley et al. (1976), Doazan et al. (1983).

An outline of the intensity variations of the Balmer emission lines (based mainly on the behaviour of H beta) is given in Figure 7. Two Balmer emission epochs have been distinguished: "epoch I", the long Be phase of strong emission ended with the 1932-1942 spectacular episode, and "epoch II", that began a few years later, at about 1946, when a new slowly increasing Be phase developed. Gamma Cas is still in this second epoch; the Balmer emission has not yet reached the preoutburst level of emission. Figure 7 visualizes the global pattern variability of Be characteristics in Gamma Cas since 1910, and demonstrates that, after nearly a century of observing Gamma Cas, it is not possible to determine any period for the variations the emission strength nor it is possible to predict the future behaviour.

In the past many authors have searched insucessfully for periodicity in different features: (a) the intensity ratio of

the violet and red emission peaks of the Balmer lines (the so called V/R variations); (b) visual magnitudes, (c) radial velocities, etc.

Also for the small and rapid profile variations, on a time scale of few minutes, detected in H-beta by Hutchings (1976) and in H-alpha by Slettebak and Snow (1978), no period has been established, and for the moment they are considered to be erratic.

Gamma Cas has been the first Be star for which super-ionized high velocity regions have been detected (Bohlin, 1970). It was observed many times in the ultraviolet region during the last decades, that is during the long Be phase which began in 1946. One of the striking results of these ultraviolet observations is that the superionized lines have varied with much greater amplitude than had the emission lines in the visible region at the same time.

Investigations from space of new spectral regions have renewed our interest in Gamma Cas also for its identification with the X-ray source MX005+63 (Mason et al., 1976).

As we have been said in the previous paragraph, Struve's rotation model is the first model that tried to explain the Be phenomenon.

The model proposed by Struve to represent the Be stars is that of a B star in rapid rotation, surrounded by a gaseous envelope which is also in rotation; the envelope is moderately dense, extended, and flattened at the equator. This model explains the diversity of the emission lines observed in Be star spectra when

it is seen under different angles of inclination of the line of sight on the rotation axis. The Be stars seen equator-on are those that exhibit a shell spectrum. If the star is viewed pole-on, the photospheric absorption lines are, on the contrary, narrow as are the emission lines which have not central reversal. If the star is viewed at an intermediate angle the emission line exhibits a weak central reversal and a Be spectrum is observed. Figure 8 is an outline of the prediction of Struve's model for H profile.

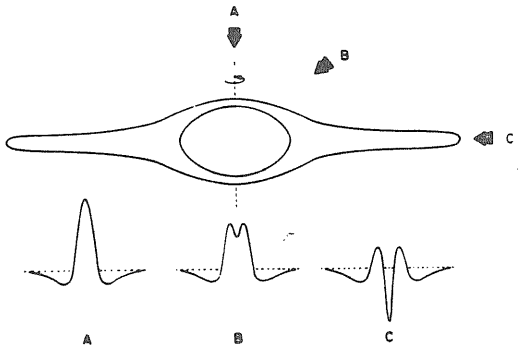

Fig.8. A schematic representation of Struve's rotation model. The different type of profiles, A,B and C, are interpreted in terms of different angles of inclination of the line of sight on the rotation axis.(from Sletteback, 1979).

Let us now apply this model to Gamma Cas and see how it works. The basic assumption of the rotation model implies for Gamma Cas a critical equatorial rotational velocity of 570 km/sec (Poeckert and Marlborough, 1978). Sletteback' s (1982) most recent Vsen i determination is of 230 km/sec, this would then

correspond to an inclination angle of about 25°.

Struve' s model attributes the broadening of the emission lines to the rotation of the envelope. Assuming that the envelope rotates, while conserving angular momentum, the width of the emission lines make it possible to compute the size of the envelope. To model the strong shell spectrum of Gamma Cas during the shell phases, we must consider an extension of atmosphere along the line of sight of 30-50 stellar radii with a mean density varying from about 10^{13} to 10^{10} cm^{-3} (Poeckert and Marborough, 1978). Thus the atmosphere of Gamma Cas, far from being very strongly confined in the equatorial plane should largely extend to high latitudes up to least 65°.

In addition the Balmer emission lines of Gamma Cas, during the episode of very strong emission, were single and very narrow i.e., at that epoch, Gamma Cas simulated the spectral appearence of a pole-on star (see fig.8 A). By contrast, during the shell phases, a few months later, the observed large emission and the deep absorption cores, simulated the spectrum of an equator-on star (see fig.8 C). During the last decade, one would infer an intermediate situation, from the double-peaked Balmer emission lines. These lines have been represented by Poeckert and Marlborough (1978), using an updated version of Struve's model, assuming an inclination angle of 45°.

At this point it is evident that the occurence of the three phases of Gamma Cas cannot be modelled with a single value of inclination angle of the rotation axis to the line of sight, under the assumptions of critical rotation and equatorial

disk-like atmospheric structure.

These difficulties encountered by the rotation model, when confronted with visual observations, are not restricted to the case of Gamma Cas.

Serious contradictions with the rotation model are also encountered when one considers the far-UV observations.

Again Gamma Cas was the first Be star whose variability was noted, even with OAO-2 at low resolution. High resolution Copernicus scans and subsequently IUE observations confirmed the variability in those lines (CIV, SiIV and NV) which are formed in the high temperature, high velocity (~ 2000 km/s) part of the atmosphere.

These expansion velocities, exceding escape velocity, have also been observed among Be stars classified as pole-on. In addition no correlation has been found between the rate of mass loss and Vsini . This implies that the mass flow is not restricted to the equatorial regions, as it is assumed in the rotation model, and there is not priviledged direction for the mass flow (Doazan et al., 1982).

These observational facts, among others, have led to propose an empirical model for Be stars where, to a first approximation, the flow is isotropic (Doazan and Thomas, 1982).

So a new empirical modeling approach has assumed the existence of the Be star variability is associated with a variable mass flow.

To conclude the comparison of the visual data and the basic assumptions and the predictions of the rotational model, we

consider the variations of the intensity ratio of the violet and red emission peaks of the Balmer lines (V/R variations). These are among the most puzzling characteristics of Be spectra. In Figure 9 are plotted the long term V/R variations in Gamma Cas. The interpretation of V/R variations is far from being satisfactory. Struve (1931), in the ambit of his model, suggested that they result from the rotation of the lines of absides of the elliptical ring. Huang (1977) gave to this idea a quantitative form representing succesfully a number of observations. Marlborough et al. (1978) have tried an explanation of Gamma Cas V/R variations by a binary motion. They postulated the existence of a compact companion revolving around Gamma Cas with an orbital period of 4 years, which is the approximate time scale of the V/R variations. Such a model would then explain both the V/R variations and the observed X-ray emission of Gamma Cas. In this model, V/R variations occur as a result of a gravitational asymmetry in the system, the envelope being more elongated towards the companion. However, in spite of long series of radial velocity measurements, no observational evidences could be found in favour of a binary nature of Gamma Cas (Cowley et al., 1976). Therefore the lack of strict periodicity of the V/R variations does not agree with this model.

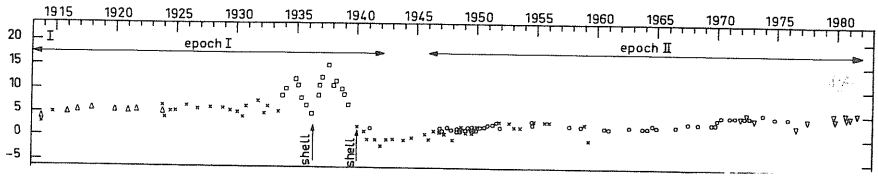

Fig.7 The long term variations of Gamma Cas in the visual region. intensity variations of the Balmer emission lines. The ordinate has an arbitrary scale, so that this figure should not be considered a quantitative representation of the emission.

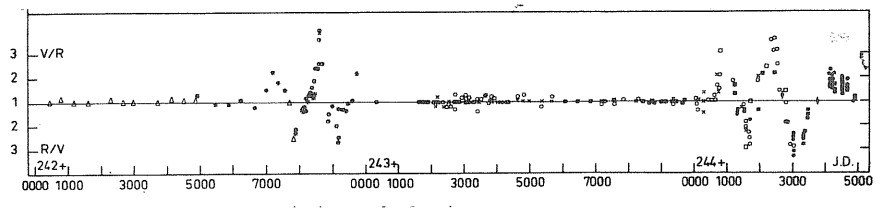

Fig.9 V/R variations of the first Balmer lines: H-delta measures , H-alpha ,H-beta (from Doazan et al.,1983 and papers therein referenced).

III OBSERVATIONS AND DATA ANALYSIS

III.1 The Observations

Here we present the observations used for check profile shape variability of the absorption lines of Gamma Cas.

All the observations were secured at the Haute-Provence Observatory during the epoch 1972-1981. We analyze here 46 blue plates obtained at the coude' spectrograph at the 152 cm telescope at 7.2 $\mathring{A}/mm^{-1}$ reciprocal dispersion. The spectral region covered ranges from 3300 to 5100 $\mathring{A}$. Kodak plate IIa0 were used.

Table 2 gives the list of spectra, the dates and times of observation.

These are a part of a series of spectra of Gamma Cas already used for analysing the main spectral features which arise in the cool H-alpha/H-beta emitting region of the outer atmosphere of Gamma Cas during the epoch 1972-1981 (Doazan et al.,1983).

TABLE 2

SPECTROGRAM	DATE(D-M-Y)	TIME(H-M)	JULIAN DAY
GC387	22 1 1972	18 26	41339.2695
GC395	24 1 1972	20 34	41341.3555
GC402	28 1 1972	18 24	41345.2656
GC403	29 1 1972	17 58	41346.2500
GC501	10 7 1972	20 2	41509.3359
GC505	14 7 1972	2 40	41512.6094
GC507	17 7 1972	2 33	41515.6055
GC509	18 7 1972	2 37	41516.6094
GC957	25 8 1976	0 55	43015.5391
GC958	25 8 1976	1 9	43015.5469
GC959	25 8 1976	1 21	43015.5547
GC960	25 8 1976	1 34	43015.5664
GC961	25 8 1976	1 59	43015.5820
GC962	25 8 1976	2 12	43015.5898
GC963	25 8 1976	2 24	43015.6016
GC964	25 8 1976	2 37	43015.6094
GC965	25 8 1976	2 47	43015.6172
GC966	27 8 1976	1 17	43017.5547
GC967	27 8 1976	1 31	43017.5625
GC968	27 8 1976	1 45	43017.5742
GC969	27 8 1976	2 00	43017.5820
GC970	27 8 1976	2 14	43017.5937
GC971	27 8 1976	2 28	43017.6016
GC993	22 7 1977	1 57	43346.5820
GC994	22 7 1977	2 10	43346.5898
GC995	22 7 1977	2 23	43346.5977
GC996	22 7 1977	2 35	43346.6094
GC997	22 7 1977	2 45	43346.6133
GC998	22 7 1977	2 54	43346.6211
GC1093	29 10 1979	18 59	44176.2930
GC1095	29 10 1979	22 43	44176.4492
GC1096	29 10 1979	22 57	44176.4609
GC1097	30 10 1979	21 17	44177.3906
GC1099	31 10 1979	21 31	44178.4023
GC1100	31 10 1979	21 44	44178.4102
GC1102	1 11 1979	20 34	44179.3594
GC1104	17 12 1979	19 42	44225.3242
GC1108	18 12 1979	20 32	44236.3594
GC1110	19 12 1979	19 40	44227.3242
GC1128	27 2 1980	22 8	44297.4219
GC1129	27 2 1980	22 17	44297.4297
GC1157	1 10 1980	0 35	44513.5273
GC1232	16 3 1981	20 8	44680.3359
GC1233	16 3 1981	20 37	44680.3555
GC1265	30 9 1981	21 29	44878.3984
GC1266	30 9 1981	21 37	44878.4062

III.2 Data Processing

All the photographic material was already digitized by means of the Perkins Elmer PDS 1010A digital microdensitometer of Naples and Trieste Observatories, and processed on the DEC PDP11/45 and VAX11/750 interactive computer system of Trieste Elspec/11 and Elspec/VMS interactive spectrograms processing packages available at the Trieste Observatory (Pasian et al., 1982).

The data processing is discussed in detail in the paper of Doazan et al., 1984.

We performed the normalization to the continuum by means a cubic spline fit of a series of selected nominal continuum points. This continuum normalization was checked by visual inspection of the data on each individual spectrum.

The sample output is shown in Figure 10, where the three helium absorption lines observed on August 25, 1976 are shown. The noise level is severe.

III.3 Data Analysis

We have measured the following lines: HeI4026, HeI4387, HeI4471 and H-gamma.

We have measured the following quantities for HeI 4026, HeI 4387

and HeI 4471 lines : a) the depth, b) the equivalent width, c) the radial velocity, d) the violet and red velocities at half depth.

The line parameters have been computed by means of the best fit of the line profile to a linear combination of one component, represented by a gaussian, with linear local continuum.

The photospheric absorption wings of the hydrogen lines, H-alpha and H-beta of Gamma Cas are never seen, during the period considered here. It is not so for H-Gamma lines, characterized by a more weak emission.

Also the parameters of H-gamma lines have been measured.These by means of the best fit of the line profile to a linear combinations of three components with linear local continuum: one component, represented by a Lorentz profile, for recostructing the photospheric absorption lines from the apparent absorption wings and two components, represented by two Lorentz profiles, for the emission of H-gamma, characterized by two peaks the violet and the red one. The best fit was applied to the linearized and continuum normalized profiles. The procedure is an improved version of the original Frazer and Suzuki (1966) technique for the optimum extimation of complex, noisy spectral lines (see appendix).

The accuracy of the line parameters depends on the noise level and the likelihood of the observed and computed lines shapes.

Sometimes more than one component is apparent in the helium absorption line profiles. This makes the parameter definition ambiguous and reduces the accuracy of the fit.

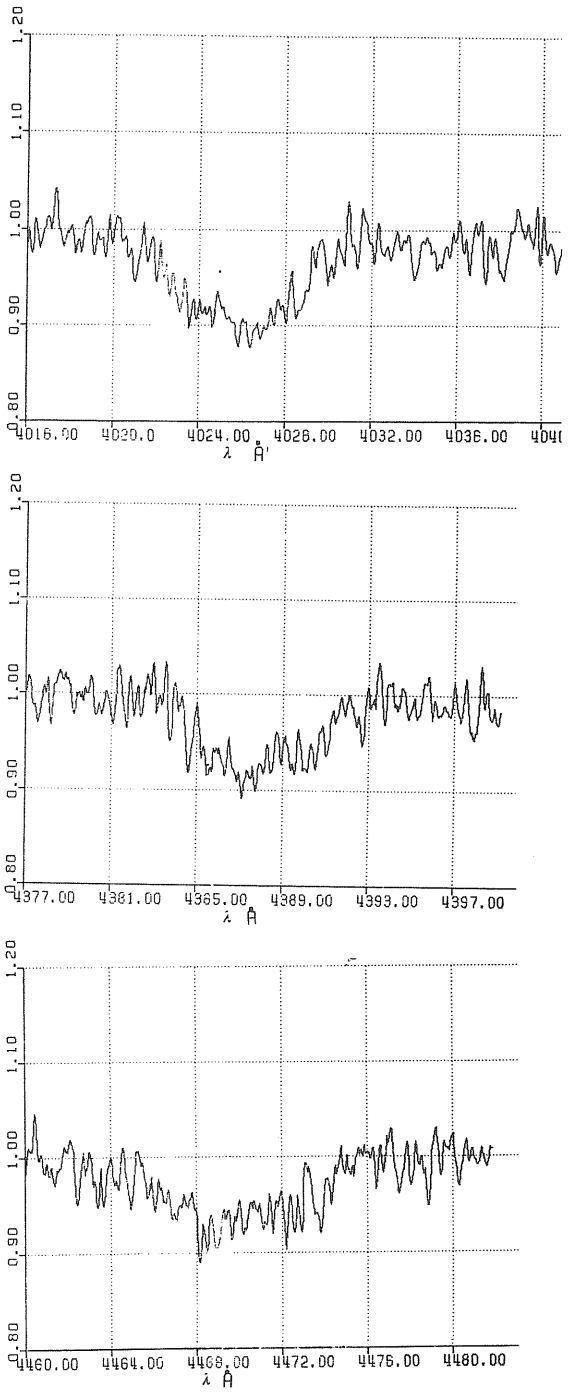

Fig. 10. The three helium absorption lines observed on August 25,1976.

IV OBSERVATIONAL RESULTS

IV.1 Short Time-Scale Variations

We have begun the analysis of the Gamma Cas spectra within a single night. We have sought support for this belief by analyzing the 6 consecutive plates taken on each of two nights, and 9 consecutive plates taken on one night (see Table 2).

The analyzed absorption lines, HeI4471 and HeI 4387 don't show pronounced asymmetries similar to that observed in the line profiles of Beta Cephei and 53 Persei stars. These Lines are very broad, the projected rotational velocity of the star on the line of sight is 230 km/sec (Slettebak,1982), and asymmetry is more easily perceivable in narrower lines.

Noticeable variations of the equivalent widths don't occur within a single night. In Figure 11 we show the equivalent widths of HeI 4471 of the series of 9 consecutive spectra extended over about 2 hours. The mean error on the equivalent width, computed from the best fit (see sec. III.3), is shown on the right hand side of the figure. This is comparable with the standard deviation of the equivalent widths.

In Figure 12 a) b) c) we show the radial velocities of the HeI4026, HeI4387 and HeI4471 line centres and wings at half depth observed during one night, the same of Figure 11.
Sinusoidal shapes of the central radial velocities and of violet and red velocities at half depth are apparent. The error on the central position, computed from the best fit, is typically about 9 km/sec for the HeI4026 lines, 15 km/sec for the HeI4387 and 13 km/sec for the HeI4471 lines. The error on the radial velocities of the wings at half depth, is typically 25 km/sec for the HeI4026, 44 km/sec for the HeI 4387 lines and 35 km/sec for the HeI4471 lines.

Because of the error on the calculated velocities, we can not assert that sinusoidal shapes, observed for the central radial velocity and violet and red velocities at half depth, are true, i.e. don't due to noise; in spite of the good correlation between the velocity of the line centres and wings in all the three helium lines observed.
The same lack of support for short term variations is given by the six spectra taken consecutively on the nights: 22-7-1979 and 29-10-1979. However we must note that they span only one hour (see Table 2).
We have already said, that the accuracy of the parameters, calculated by means of the best fit method, depends on the observed and computed lines shapes and on noise level. And the noise level of our photographic observations is severe (see Figure 10). However distortions in the line profiles are apparent in several cases, indicating that more than one

component can form the absorption line profile.

As it has been already stated our best fit computations take into consideration only one component, represented by a gaussian.These distortions, that appear and disappear across the line profiles are less marked but similar to the detected emission-assorption "bumbs" in the line profiles of non-radial pulsating stars. We have tried to examine if they are true or due to the noise by calculating the residuals for the series of 9 and 6 consecutive spectra: i.e. we have calculated the residual as individual spectra minus the mean spectrum and estimated their standard deviations.

The results are the following:

(1)we don't detect variations of the continuum normalized spectral intensity above .03 (the average continuum normalized intensity standard deviation is about .01);

(2)the line profile distorsions don't involve many pixels. So we cannot conclude that the observed distorsions due to true variations.

III.2 Long Time-Scale Variations

The observations considered here span the years 1972-1981. In order to describe the spectroscopic changes of Gamma Cas we have distinguished ten epochs of observations, each listing not more than 4 days. (1)and (2) For 1972; (3) for 1976; (4) for 1977;

(5) and (6) for 1979; (7) and (8) for 1980; (9) and (10) for 1981.

The radial velocity (square) and the violet and red velocities at half depth (triangles) of HeI4026, HeI4471 and HeI4387 are plotted in Figure 13a, 13b and 13c respectively. The data are mean values for each epoch. The calculated errors on the radial velocities of the line centres and on the position of the wings at half depth are plotted on the rigth side of Figures 13a),b) and c).

Figures 13 reflect two kinds of variations: (i) a variation of the central position of the whole absorption line, and (ii) a variation of the absorption line widths. The scatter of the radial velocities measured by the standard deviation is 27 km/sec, 35 km/sec and 30km/sec for the HeI4026, HeI 4387 and HeI4471 respectively, that is about 7, 5 and 6 times the average of the radial velocity error (see Figure 13 a),b) and c) on the right).

The HeI4026 and HeI4471 central position variations are correlated (probability 99.5%). On the contrary there are not correlation among the HeI4387 central position variations and those of the other two helium lines.

Figures 13 show that in 1976 there was an increase in the widths followed by a drop up to about the 1972 value. And this trend is common to all the three helium lines.

The depths of the three neutral helium lines can be assumed constant in the period considered here. In Figures 14 a), b) and c) the calculated depths and the relative errors are shown.

Figures 15 a), b) and c) show the variations of the equivalent width of the three helium absorption line.
It is seen that there is an increase in equivalent widths in the 1976, followed by a drop up to about the 1972 value, in 1979-1981.
The behaviour of the absorption line HeI4387 (Figure 15 b) is not so clear. This line is shallower than the other two helium lines, and in some spectra ill-defined.

The increase in the strengths of the helium absorption lines in the 1976 is correlated with a drop in the emission strength of H-beta lines occuring during the same period. Figure 16 shows the variations of the emission strength at H-beta in the period considered here (from Doazan et al., 1983). It seen that there is a drop in intensity from 1973 to 1976 followed by an increase up to about its 1973 value in 1979-1981.
We have also measured the photospheric absorption wings of H-gamma lines. We have already said that the H-alpha and H-beta absorption wings are never (or very badly) seen during the period considered here, but the H-gamma lines are characterized by a more weak emission which allows us to measure a good fraction of line wings.
The error on the calculated depths, of the H-gamma absorption lines is 2.6%. An increased signal to noise ratio has been achieved by performing the average of the single spectra at each epoch.
The increase in the strengths of the helium absorption lines in the 1976 is correlated in time with the increase of the

equivalent widths of the H-gamma absorption lines.

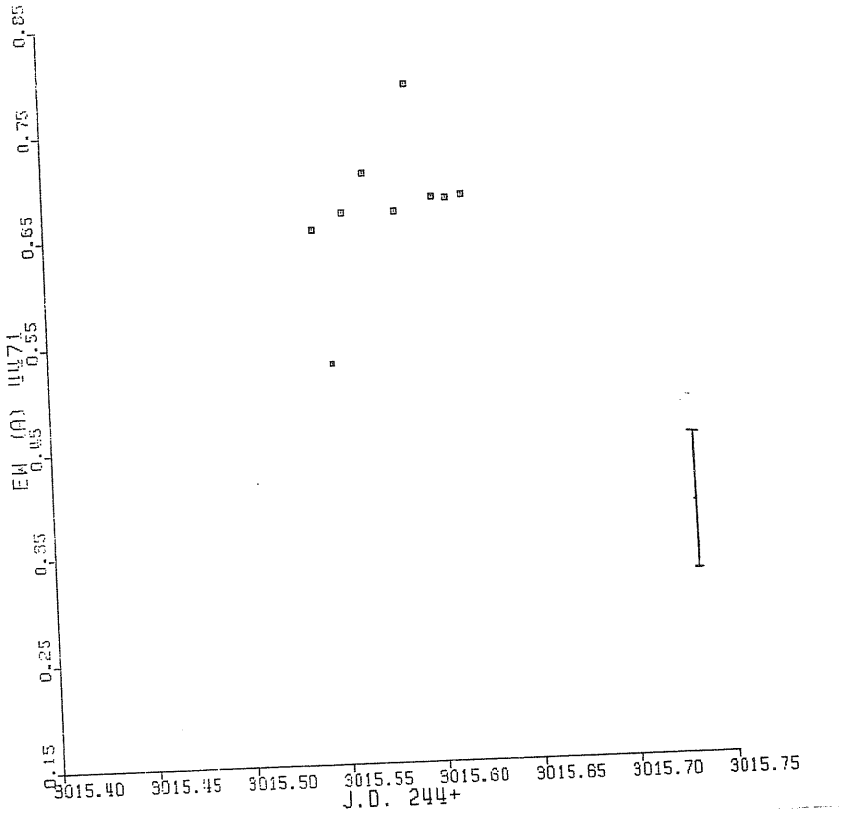

Fig.11. See text.

Fig.12 a). See text.

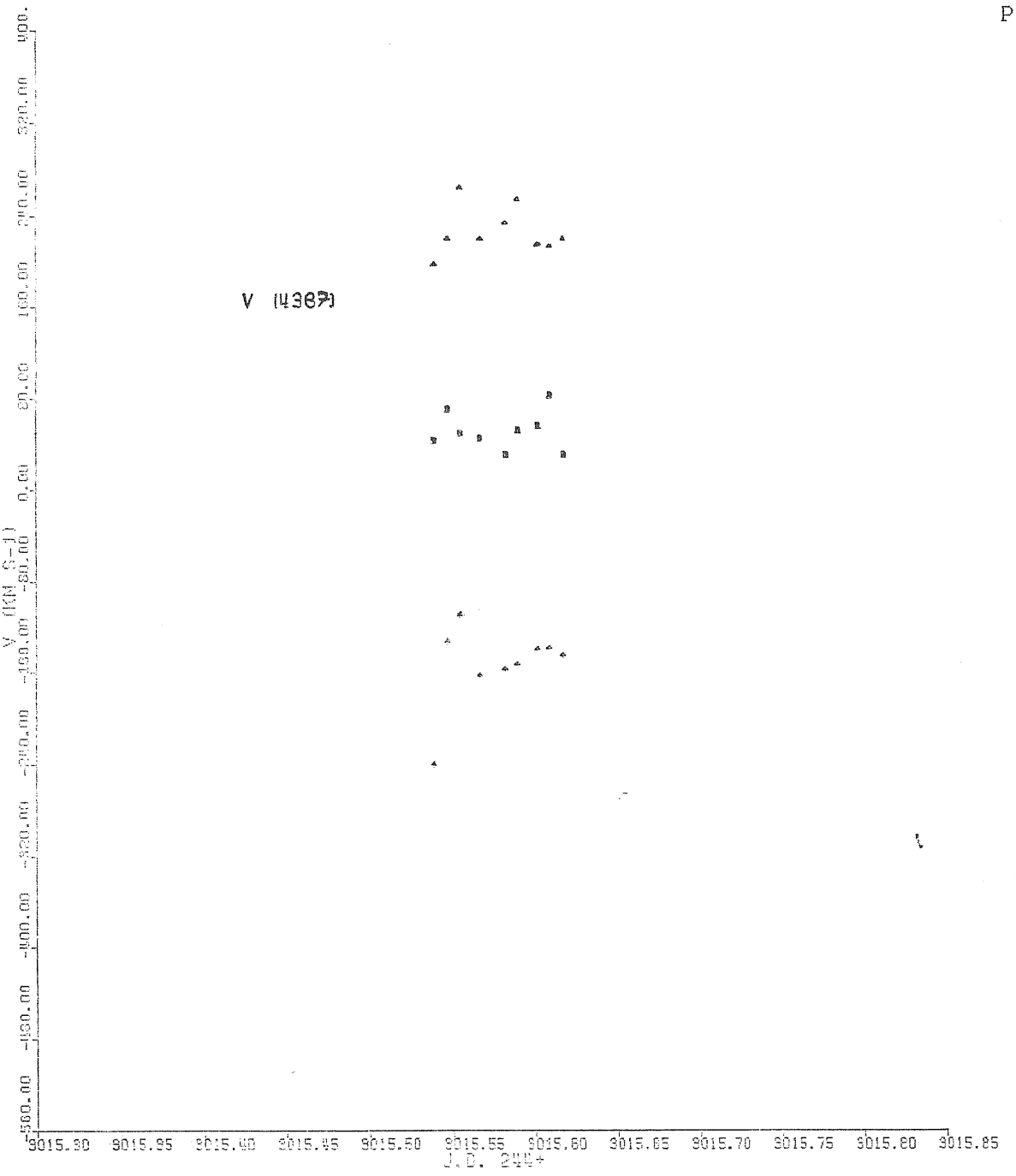

Fig.12 b). See text.

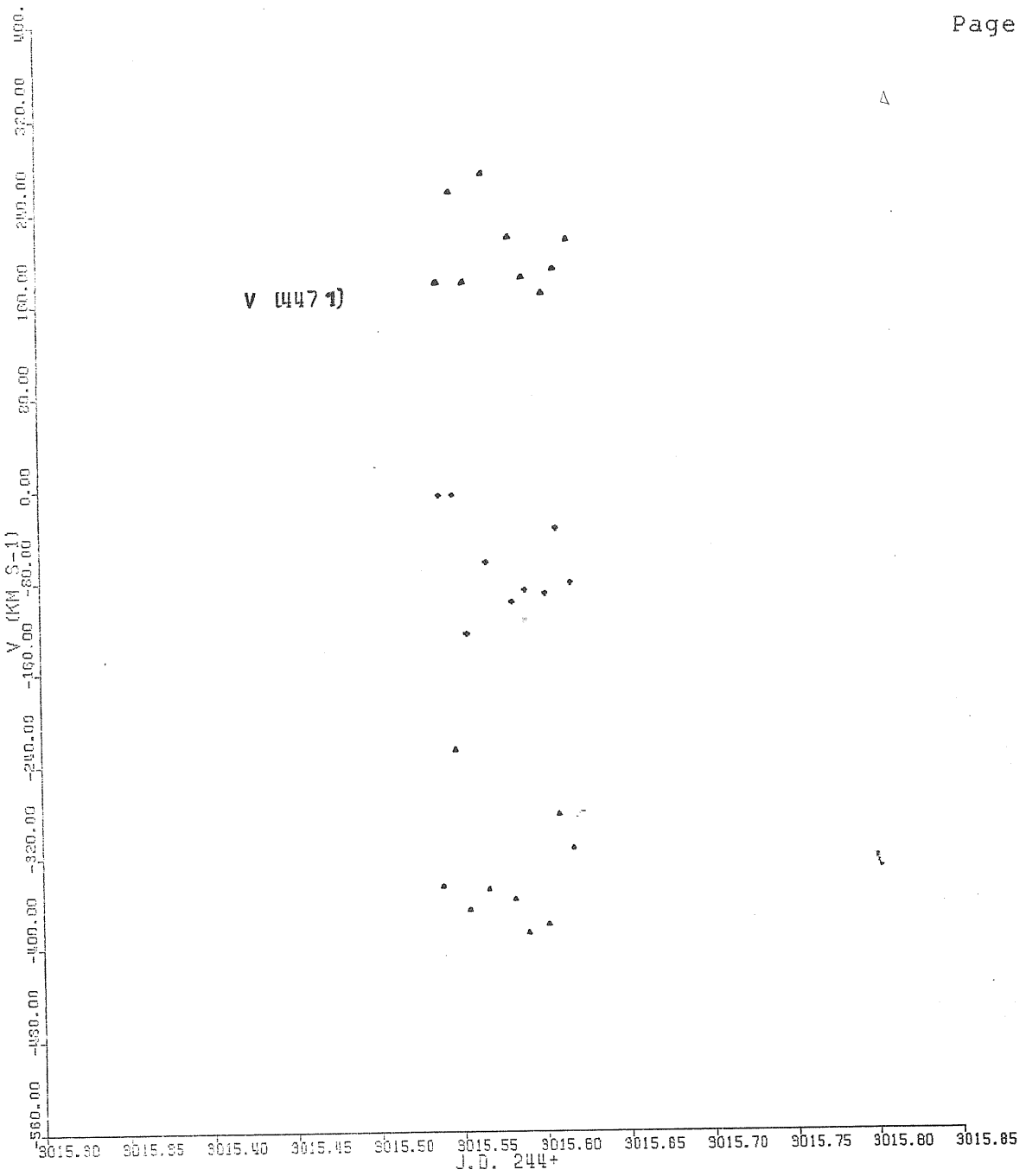

Fig.12 c). See text.

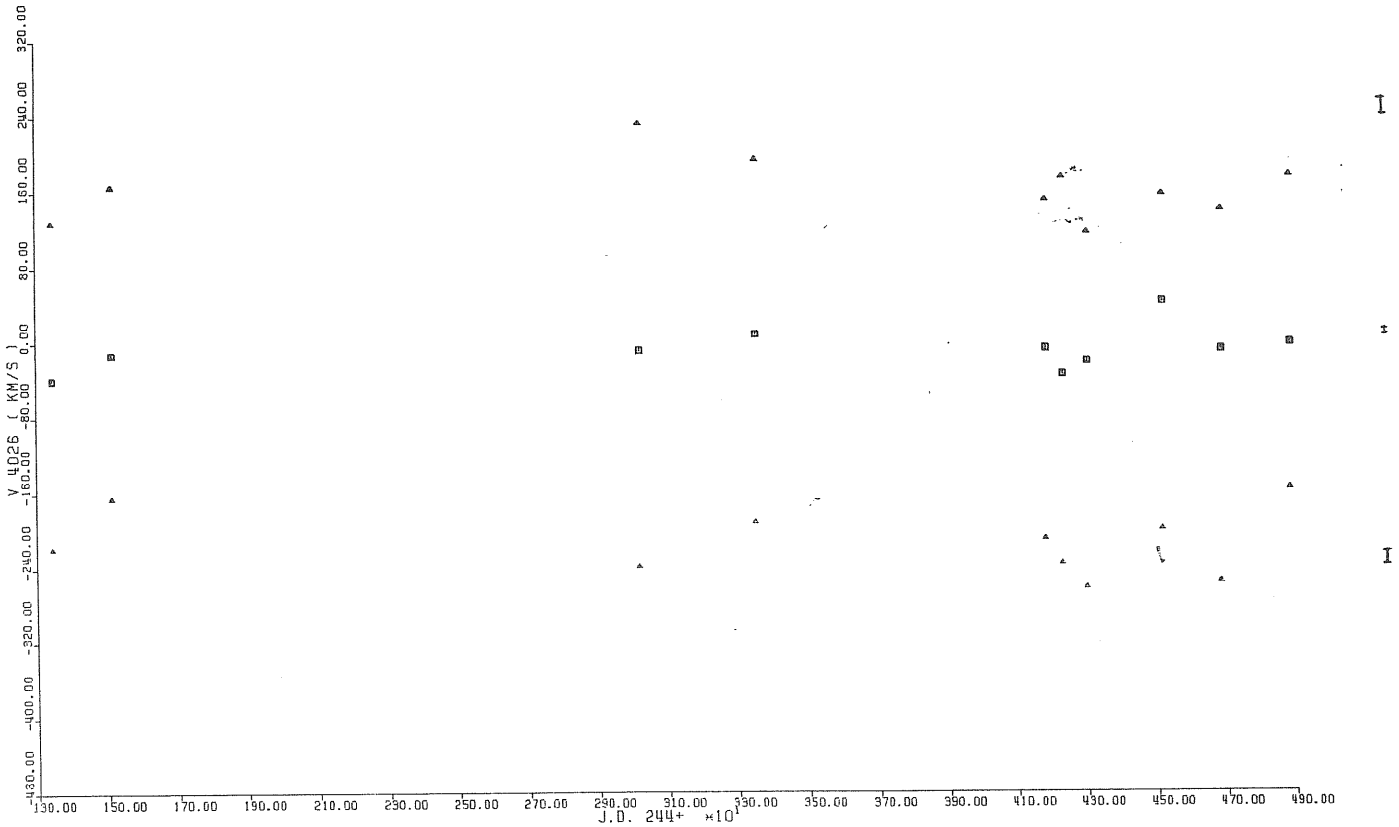

Fig.13 a). See text.

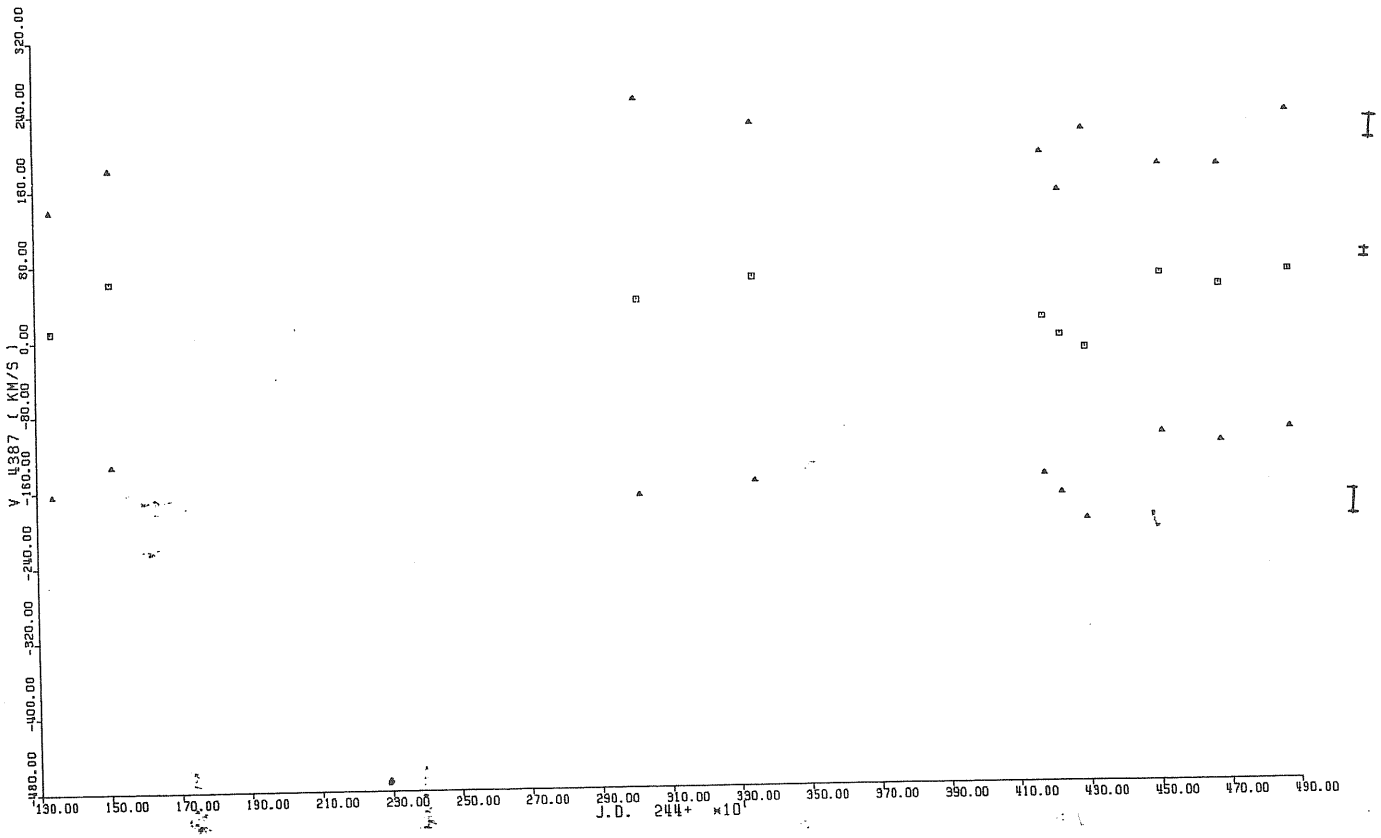

Fig.13 b). See text.

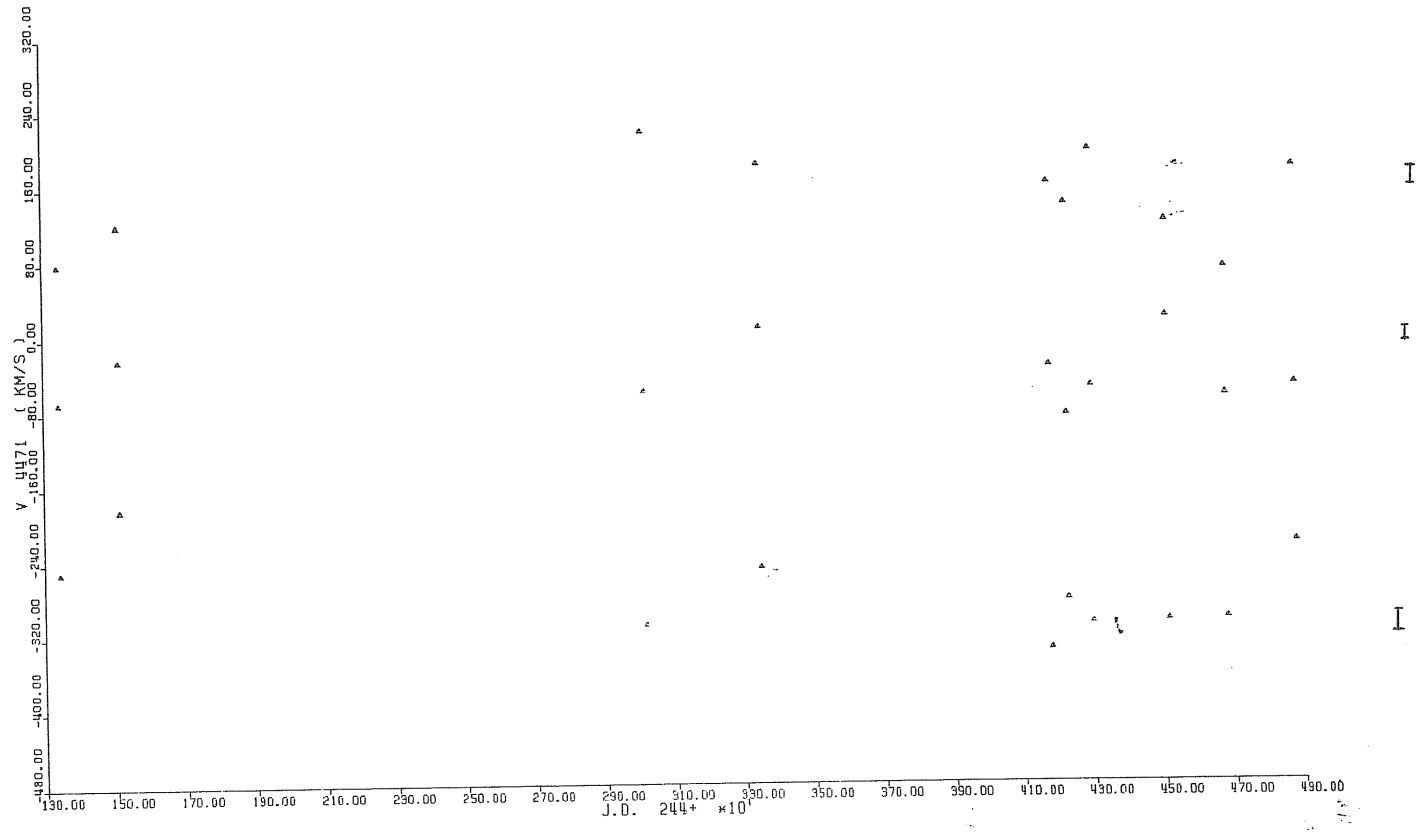

Fig.13 c). See text.

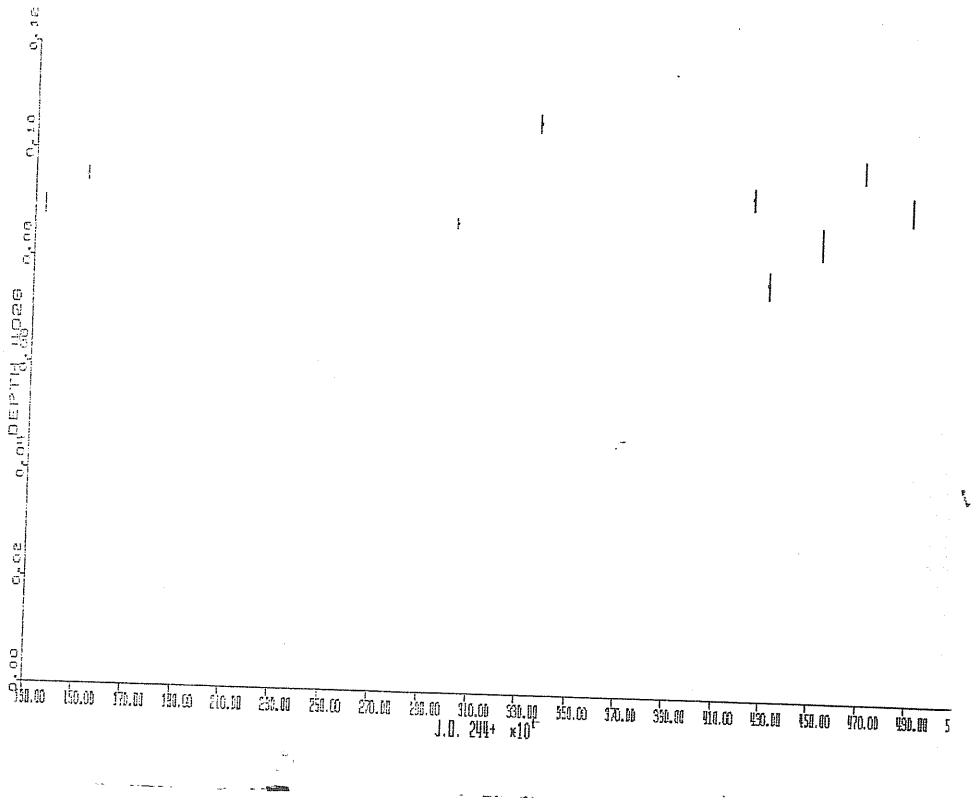

Fig.14 a). See text.

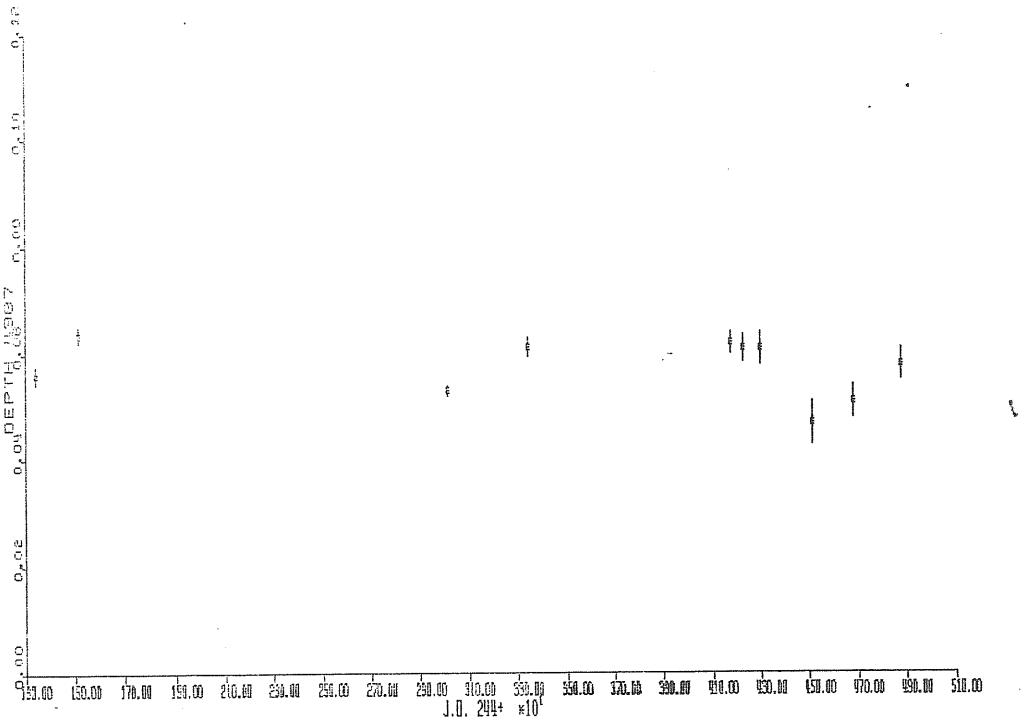

Fig.14 b). See text.

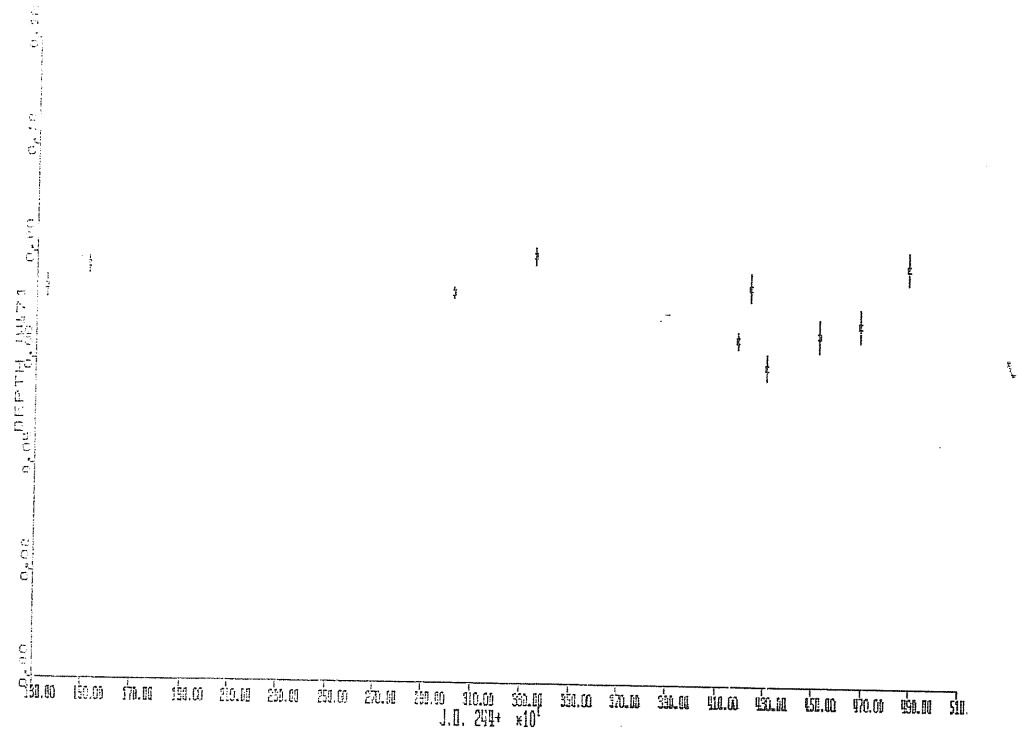

Fig.14 c). See text.

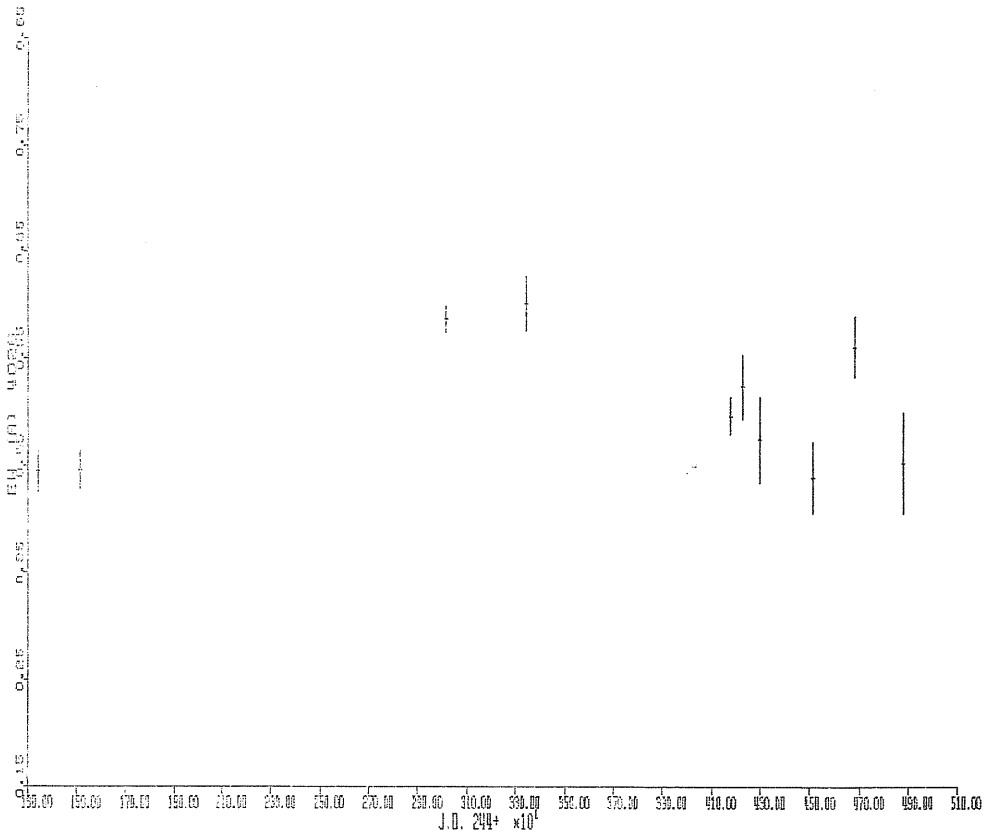

Fig.15 a). See text.

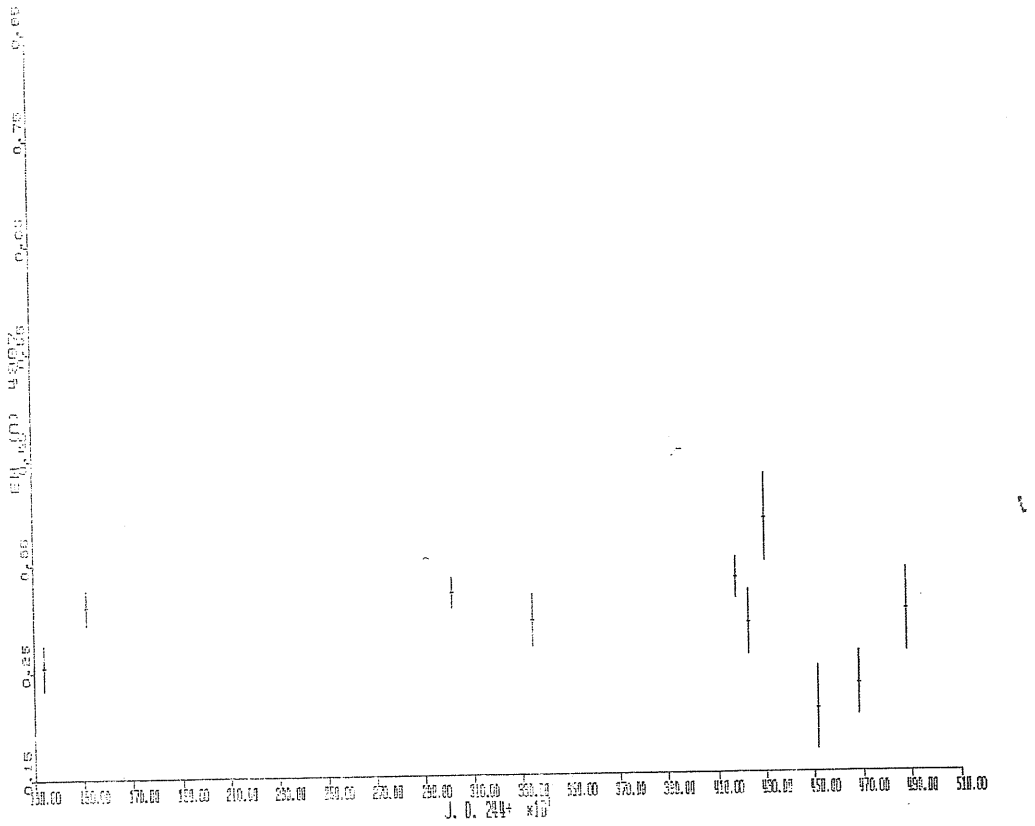

Fig.15 b). See text.

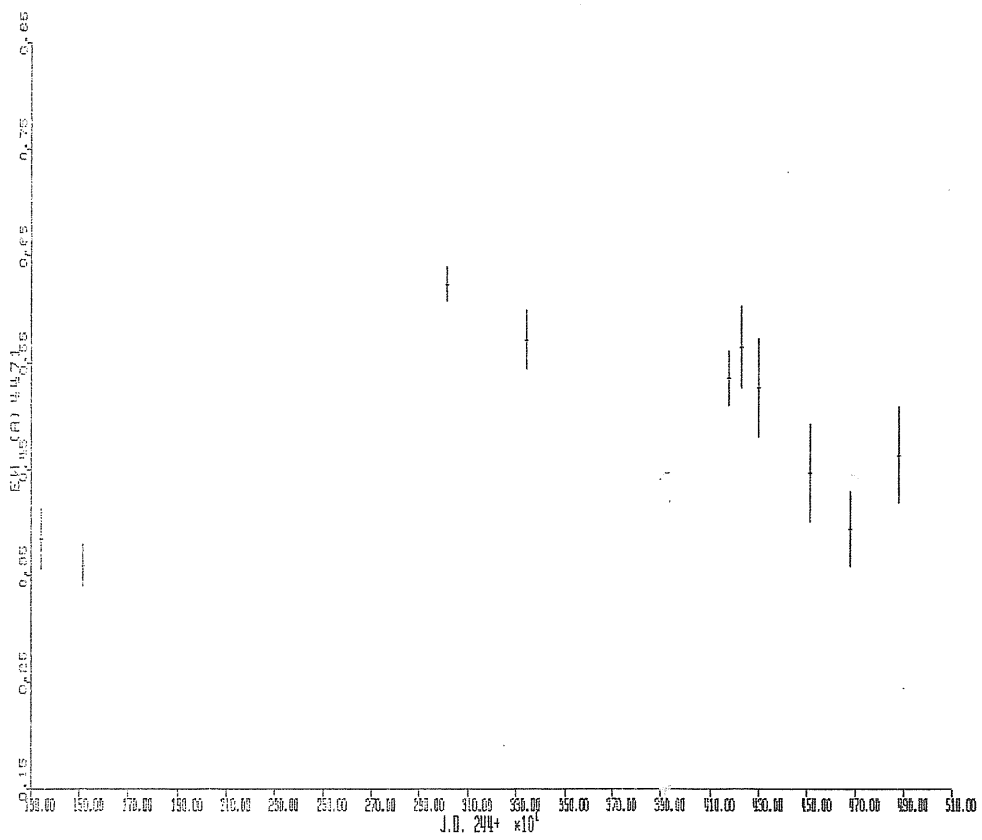

Fig.15 c). See text.

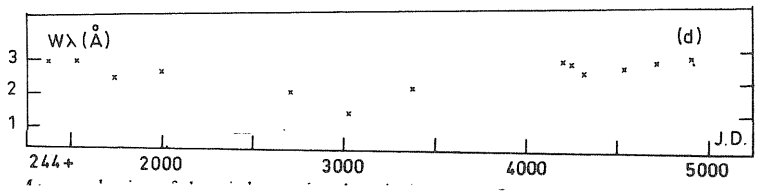

Fig.16. Variations of the emission strenght at H-beta (from Doazan et al., 1983)

V DISCUSSION AND CONCLUSIONS

V.1 Short Time-Scale Variations

Rapid variations of the photospheric lines have not been detected in our data set. The reason should be that, despite the excellent quality of our spectroscopic material, the noise level of photographic observations makes difficult to detect and measure asymmetries or "bumbs", similar to those which are detected in line profiles of other pulsating stars, when the observations are made with electronic detectors.

V.2 Long Time-Scale Variations

In this section we confront the characteristics of the long-term variations of the emission and absorption lines of Gamma Cas in the visual with the basic assumptions of the Gamma Cas models.

i) Radial velocities and binary model of Gamma Cas.

As reported in section II.2 Marlborough et al. (1978) proposed binary model for Gamma Cas. They postulated the existence of a

compact companion revolving around the star with orbital period of 4 years.

Cowley et al. (1976), in spite of a long series of radial velocity measurements, did not find observational evidences in favour of a binary nature of Gamma Cas. They measured radial velocities in 92 spectra, taken during the period 1933-1942, and searched for possible periods in the range between 2.5 ^{d} and 4000 ^{d}.

Our measurements of radial velocity have been made on the three helium lines only. The HeI4026 and the HeI4471 are doublets with forbidden component. The HeI4387 has the lowest quality among the lines studied here. Figures 13 show the different trend of the variations of the HeI4387, compared to those of the other two helium lines, it can be explained by the different molteplicity of the term. Thus we can not find absolute values for the radial velocities. Therefore it is not possible to find a periodicity for the observed radial velocity variations for lack of sufficient complete time coverage of the observations.

ii) Line intensities and "envelope" model of Gamma Cas.

We have already said that the variations of the strengths of the helium and H-gamma absorption lines are correlated in time with the emission strengths of H-beta lines.

In Table 3 we summarize the qualitative behaviour of the Gamma Cas line strengths, in the period considered here. The first epoch has been taken as reference. A departure of the line

strength from its reference value is given by an upward arrow, if there is an increase and by a downward arrow, if there is a decrease. The length of the arrows is approximately proportional to the departure from the reference value. If there is not departure we use the symbol, ~. For semplicity, we have averaged the results of the last six epochs, that span from 1976 to 1981, in two epochs.

TABLE 3

Epoch	I	II	III	IV	V	VI
H-beta emission lines*	~	~	↓	↓	↓	~
H-gamma absorption lines	~	~	↑	↑	~	~
HeI 4026 HeI 4471 absorption lines	~	~	↑	↑	↑	↑
HeI 4387 absorption lines	~	↑	↑	~	↑	~

* From Doazan et al., 1983.

The correlations presented in Table 3 between the increase in strength of the absorption lines and the drop of the emission intensity and the fact that both photosphere and envelope

contribute to the line spectrum, suggest the following question: What is the source of variability?

That is, we ask if the observed variations in the absorption line strengths are caused by photospheric changes, or by envelope variability.

The envelope can be the source of equivalent width variations of the HeI lines, if undetectable (to our instrument) variable emission is present in these lines.

In a simple photosphere/wind/envelope scheme (as that supposed by Doazan and Thomas, 1982) such emission should form in the ~10000 °K H-alpha forming envelope, thus, should be correlated in strength and time with the hydrogen line emission. A general decrease of the emission strength might cause an increase in the neutral helium absorption lines. We indeed observe that the increase in the strength of the helium absorption lines in 1976, is correlated in time with a drop in the emission strength of the H-beta lines (see table 3). As a further support for this interpretation we note that at the epoch 3 some helium lines show evidence of an emission feature in the red side (see Figure 17). At that epoch the intensity ratio of the red to violet emission peaks of the H-beta lines is maximum, according to Doazan et al. (1983) paper. Note that the emission feature is detected on the red wings only because at the epoch 3 we are in a phase of R/V >> 1. When viceversa the H-beta red emission peak is lower than the violet one we don't detect any evidence of emission in the blue part of the He4471 lines. An explanation of this lack of emission is that our data set does

not include period of very strong V/R ratio.

The possible alternative is that the observed variations in the absorption line strength are not caused by only envelope variations (due to phenomena related to mass loss and/or dishomogeneities in the outer structure of the envelope) but by a global change on the overall atmospheric structure of the star. This change can take origin in the sub-photosphere, and propagate through the photosphere possibly out to the envelope. Under this second hypotesis the emission feature that we detect in the HeI4471 lines is only a secondary effect of the envelope on the photospheric spectrum.

In order to check this alternative hypotesis, we have tried to estimates Gamma Cas effective temperature and gravity at the different epochs. Namely: (1) H-gamma wing profiles (we measure the wings because they are unaffected by the central emission in H-gamma); (2) ratio HeII/HeI equivalent widths.

With the absorption lines of H-gamma (wings), HeI and HeII available for analysis one has, in principle, enough informations to determine the fundamental atmospheric parameters: effective temperature (essentially from the ratio of HeII to HeI line strengths), and surface gravity (essentially from the H-gamma wings). In particular in the O and B0 stars for which the lines of both HeI and HeII are observable the HeI/HeII ratio is a very good temperature criterium. Also the spectral energy distribution in the range 912 A to the IR gives information on the effective temperature.

In Figure 18 and 19 theoretical equivalent widths of HeI4471 and

HeII4686, are plotted as a function of effective temperature and gravity. They are the result of an extensive series of LTE and non-LTE calculations of the H, HeI and HeII spectra of O and B stars that was carried out by Auer and Mihalas in 1972, using relatively complete atomic models, allowing for many levels. We see that both LTE and non-LTE calculations show a monotonic decrease in line strength of the HeI4471 line with increasing temperature and a correspondent increase on the HeII4686 line strength. In the spectrum of Gamma Cas the HeII4686 line is shallow and ill-defined. So the ratio of HeII to HeI line can hardly give any information on the effective temperature changes during the period of observation.

Informations, essentially on the surface gravity, can be obtained from the H-gamma line wings.

Comparing the H-gamma line wings with computations of H-gamma profiles by non-LTE atmospheric models, that have been performed for effective temperature in the range 20000°K - 35000°K and gravity in the range $3*10^{2}$ - $3*10^{4}$, by Mihalas in 1972, we obtain in the effective temperature-gravity plane the curves that are plotted in Figure 20. One curve for each epoch, where we have averaged the results of the last six epochs, that span from 1976 to 1981, into two epochs because there were not measurable variations in the profiles observed during the epochs 5,6,7 from one side and 8,9,10, from the other. The two dashed curves indicate the error on the first-epoch curve. Similar curves can be established for the other epochs.

Thus according to these error estimates, there is a change in

the location of iso-profile curves between epoch I and III/IV. At epoch VI the iso-curve recover the epoch I value.

If we assume a constant effective temperature for Gamma Cas at the T_{eff} =29000 °K value given by Underhill (1982), in her effective temperature scale for B0.5 IV stars, then the changes in the iso-curves correspond to a passage from log(gravity)=3.3 (epoch I) to log(gravity)=3.5 (epoch III/IV) through a possible intermediate value during epoch II, and a return from log(gravity)=3.5 to the original 3.3 value at the epoch VI, through a possible intermediate value during epoch V. These results seem to be confirmed even for the variations in the line strenghts of the helium lines (see Figure 21 for the HeI4471 lines). Again as for the H-gamma wings we have averaged epoch 5,6,7 together as well as epoch 8,9,10.

Viceversa if we keep the gravity constant at the value log(gravity)=3.4, which is compatible with our main sequence rotating star, then the change of the iso-profile curves obtained from our H-gamma data gives a sequence of temperature between epoch I and III/IV from 27500°K to 30000°K, and back again at epoch VI.

Unfortunately the ratio HeII/HeI does not give any support to this temperature variations. In our range of effective temperature, model atmosphere predicts equivalent width of HeII lines less then .03 Å, at ours signal to noise ratio level, and at the rotational velocity of Gamma Cas we cannot obtain reliable measurements of such values of equivalent widths.

In conclusion we support these 2 possibilities for the long

term, slow changes of the physical conditions in Gamma Cas, during the period considered here.

1)It is possible that both effective temperature and gravity change giving us the spectroscopic signature of these variations through the H-gamma and HeI photospheric lines. The origin of these changes is not known. They could be linked to the "binary" character of the star proposed by Poeckert and Marlborough (1978);or to an unknown mechanism occuring in the subphotosphere and related to the Be phenomenum. There are indeed several evidence in the Be stars of similar variations (Doazan et al.,1985, Polidan et al., 1985).

2)It is possible that the physical conditions of the envelope change, as observed from the H-alpha and H-beta emission lines. The absorption line variations can be due to residual emission from the envelope, which changes according to the H-alfa, H-beta lines. The origin of the change are very likely related to variable mass loss rate which is characteristic of many Be stars.

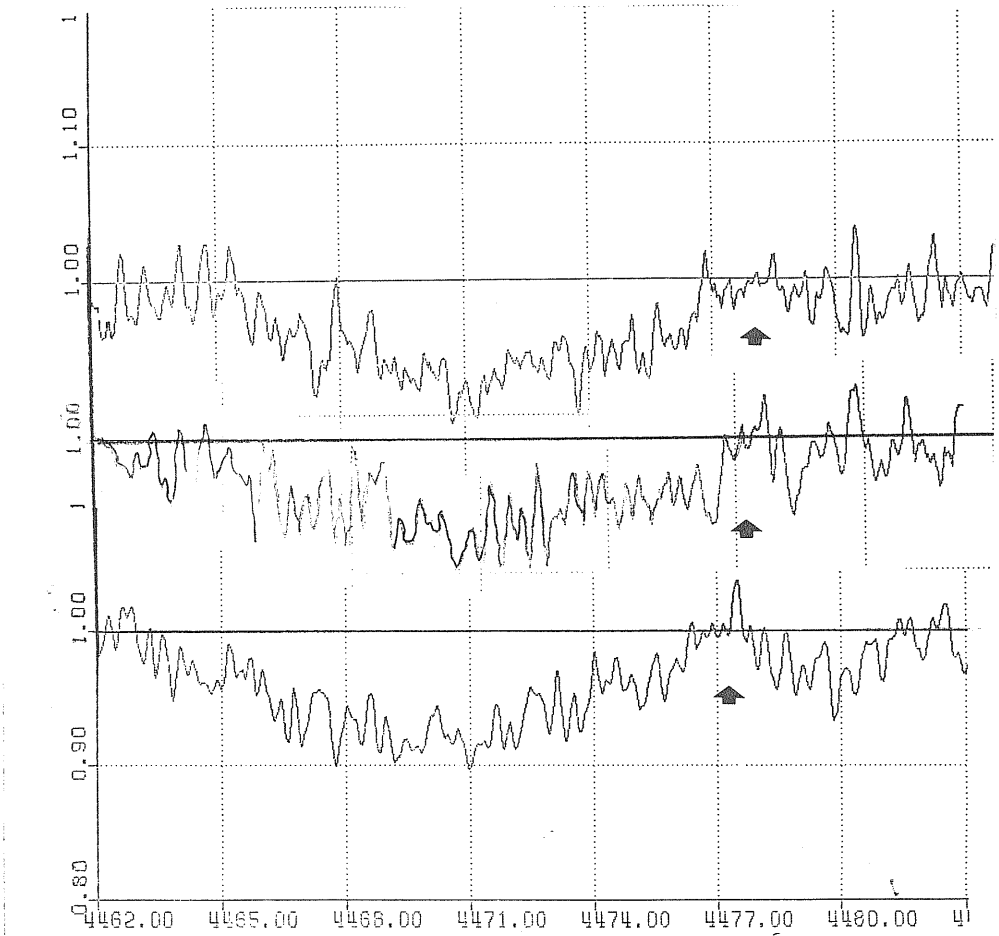

Fig.17. HeI absorption lines observed in 1976. The arrows indicate the emission features.

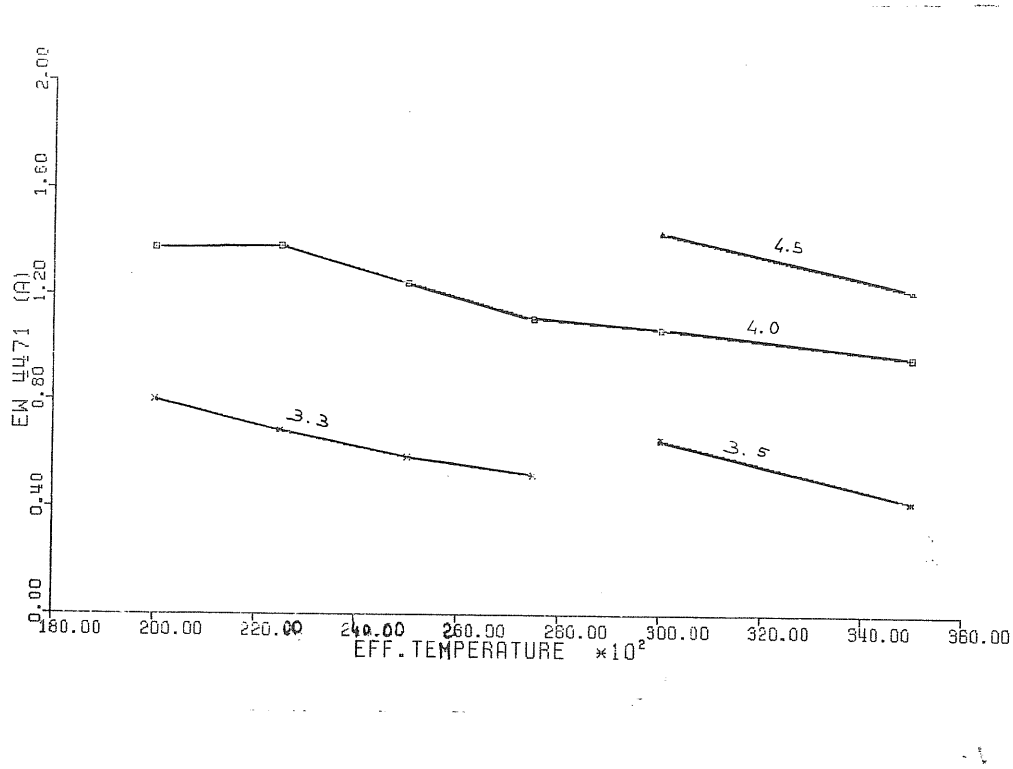

Fig.18. Equivalent width of the HeI4471 as a function of the effective temperature . Curves are labeled with log g (NLTE models from Auer and Mihalas, 1972).

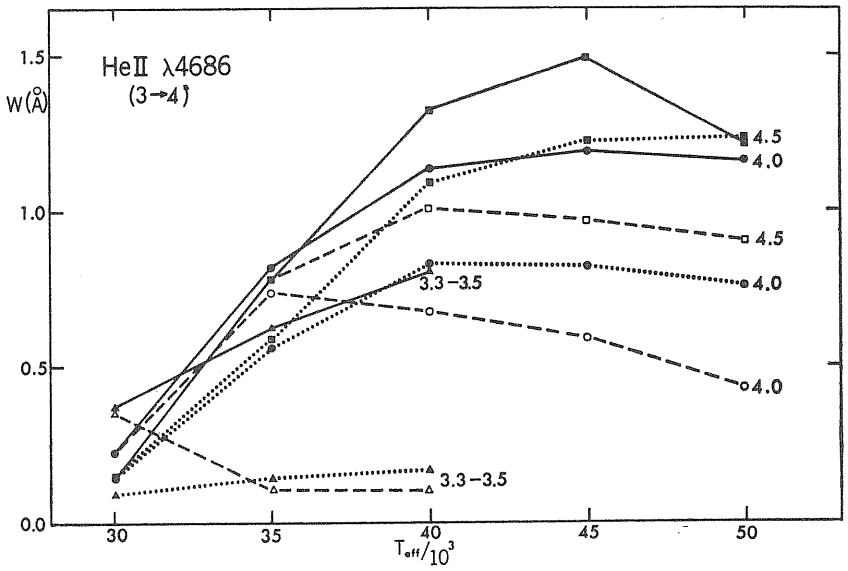

Fig.19. Equivalent widths of the HeII4686 as a function of the effective temperature. The curves are labeled with log g; solid curves with solid symbols refer to NLTE/l models (no overlap with H lines), and the dotted curves with solid symbols refer to NLTE/f models (complete overlap with the H lines) (From Auer and Mihalas, 1972).

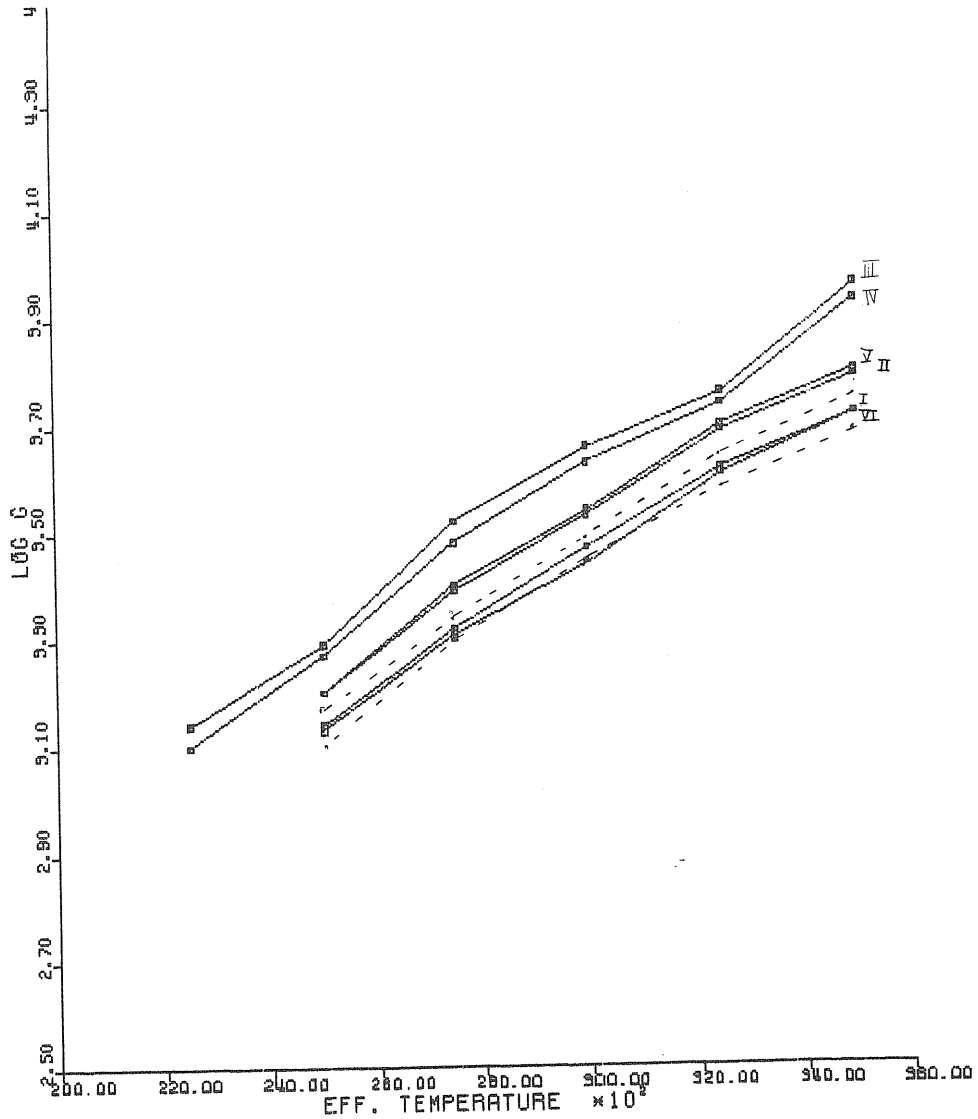

Fig.20. See text.

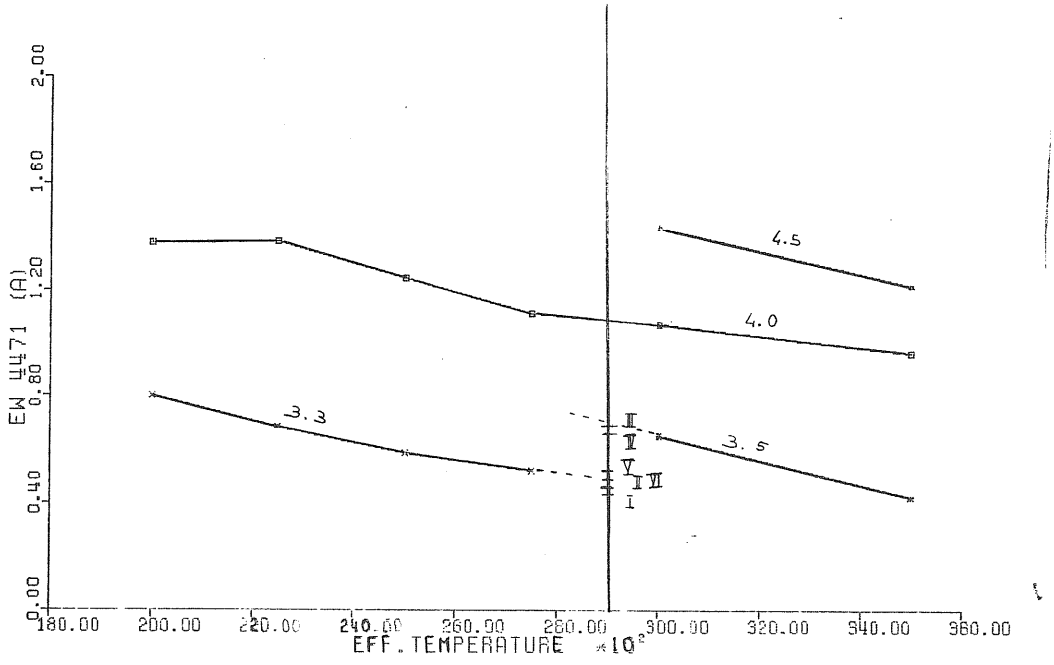

Fig.21. See text.

APPENDIX

In the present appendix the theory of the Frazer and Suzuki (1966) technique for the optimum estimation of complex, noisy spectral lines is outlined.

Our data are in the form of a list of points (x_i, y_i), i=1,.....,n., where x are the wavelengths and y_i the corresponding normalized intensities. The function F(x) which is to be fitted to these data will contain a number of parameters $P_1, \ldots\ldots\ldots, P_m$, which define a system of bands and a baseline, the aim is to choose values for the parameters which give the best representation of the observed data. We can assign a weighting function, w_i, proportional to the relative importance or reliability of the i^{th} observation. Frequently all the data points are given equal weight.

A convenient criterion of goodness of fit is the mean square deviation between the calculated and observed y_i values, that is the quantity

A1.1
$$\langle \varepsilon^2 \rangle = \frac{\sum_i^n w_i \left[F(x_i) - y_i \right]^2}{\sum_i w_i}$$

The quantity $\langle \varepsilon^2 \rangle$ will, in general, contain three components: one due to the noise level of the y_i values, a systematic component due to the difference between the actual and assumed band functions.

Therefore it is a function of all the parameters, it is assignment of the least square method to furnish the values of $P_1, \ldots, P_m$, such to minimize this component.

The problem of choosing $P_1, \ldots, P_m$ so as to minimize $\langle \varepsilon^2 \rangle$ is greatly simplified if approximate values $P_1^\circ, \ldots P_m^\circ$ can be guessed, the adjustments $\Delta P_j^\circ = P_j^\circ - P_j$ required to optimize the parameters may then be calculated by the following method.

Using Taylor's expansion, and neglecting second and higher order terms, we obtain the following expression for $F(x_i, P_1, \ldots, P_m)$:

$$\text{Al.2} \qquad F(x, P_1, \ldots, P_m) = F(x, P_1^\circ, \ldots, P_m^\circ) + \sum_{j=1}^{m} \frac{\partial F}{\partial P_j}(x_i, P_1^\circ, \ldots, P_m^\circ)\, \Delta P_j^\circ \qquad (i=1, \ldots, n),$$

more concisely

$$\text{Al.2} \qquad F_i = F_i^\circ + \sum_{1}^{m} \left(\frac{\partial F_i}{\partial P_j}\right)^\circ \Delta P_j^\circ$$

This type of procedure has only a local validity.

The condition that $\langle \varepsilon^2 \rangle$ is a minimum requires that $\frac{\partial \langle \varepsilon^2 \rangle}{\partial P_j} = 0$, with $j=1, \ldots, m$, that is

$$\frac{\partial}{\partial P_j} \sum_{1}^{n} w_i \left[F(x_i, P_1, \ldots, P_m) - y_i \right]^2 = 0 \qquad (j=1, \ldots, m).$$

And if the expression for F_i in eq. Al.2 is substituted in eq. Al.1, a set of simultaneous equations for the parameter adjustments is obtained by equating each of the m partial derivatives of $\langle \varepsilon^2 \rangle$ to zero,

$$\text{Al.3}\quad \sum_{i}^{m} \Delta P_j^{\circ} \sum_{i}^{n} w_i \left(\frac{\partial F_i}{\partial P_j}\right)^{\circ}\left(\frac{\partial F_i}{\partial P_k}\right)^{\circ} = -\sum_{i}^{n} w_i \left(F_i^{\circ} - Y_i\right)\left(\frac{\partial F_i}{\partial P_k}\right)^{\circ}$$

$$(k=1,\ldots\ldots,m).$$

Expression Al.3 is much simpler than it appears; the set of equations can be written in the following matrix form:

$$\text{Al.4}\qquad [\,C\,]\,\underline{\Delta P}^{\circ} = \underline{d}\quad , \text{ where}$$

$$C_{jk} = C_{kj} = \sum_{i} w_i \left(\frac{\partial F_i}{\partial P_j}\right)^{\circ}\left(\frac{\partial F_i}{\partial P_k}\right)^{\circ}\quad ,$$

and the vector d has components:

$$d_k = -\sum_{i}^{n} w_i \left(F_i^{\circ} - Y_i\right)\left(\frac{\partial F_i}{\partial P_k}\right)^{\circ}$$

$$(k=1,\ldots\ldots,m)\ .$$

Al.4 can be solved by using readily avalaible computer subroutines, which require the C and d as input and return the values of $\Delta P_1, \ldots\ldots, P_m$.

$$\text{Al.5}\qquad \underline{\Delta P}^{\circ} = [\,C\,]^{-1}\,\underline{d}\quad .$$

The optimum values of the parameters will be:

$$\text{Al.6}\qquad P_j^{1} = P_j^{\circ} + \Delta P_j^{\circ}\qquad\qquad (j=1,\ldots\ldots,m).$$

As F(x) is not a linear function of the parameters, Eq. Al.2

gives only an approximate value for $F(x_i)$, and the computed parameter adjustments will not be exactly those required to correct the trial values. If the calculation is repeated using the adjusted parameters in place of the original trial values, a further refinement will be obtained, and by repeated cycling the optimum values of the parameters may be calculated to a degree of accuracy limited by noise level and modelling errors.

The goodness of fit, after each cycle, can be calculated by the root-mean-square deviation between the calculated and observed y values. This quantity, in favorable circumstances, decreases rapidly with successive cycles of refinement, and the optimization procedure can be terminated when additional cycles do not produce any significant change in the values of the parameters. That is when all the parameter adjustments, ΔP_j, are less than the root-mean square deviation between the calculated and observed value the procedure can be terminated. In such cases the process is said to converge.

If the trial values of the parameters are an extremely poor approximation to the correct value the process can diverge. A caracteristic of this situation is that the calculated parameter adjustments are very large, and they lead to worse rather than better estimates of the parameters. A method of preventing divergence is to minimize the following expression, instead of the Al.1,

$$S=\sum_{i}^{n} w_i [F(x_i, P_1, \ldots\ldots, P_m)-y_i]^2 + D^2 \sum_{j}^{m} A_j (\Delta P_j)^2 ,$$

where the coefficient D, which is chosen empirically, is called the damping factor, and the only modification required to equation A1.4, to solve the problem, is to multiply the diagonal coefficient of the matrix C, C_{jj}, by $(1+D^2)$.

When the refinement has been carried out the required degree of accuracy, the deviations between the observed value and the fitted value will be distributed normally.

The magnitude of $\langle \varepsilon^2 \rangle$, calculated in according to eqation A1.1, will in general contain a component due to the random errors of measurement in the y values together with a systematic component due to the difference between the real and assumed function, $F(x_i, P_1, \ldots\ldots, P_m)$ assumed to fit the observed data.

F(x) will be of the form:

A1.7 $$F(x) = \sum_{t=1}^{n_b} G_t(x)+B(x) ,$$

where G_t are n_b functions, each of wich contains parameters describing a band, and B is a function which generates a base line. If a particular form of G(x) is predictable from theoretical considerations, then this form should of course used.

Two types of function are often encountered in the dealing with absorption spectra: the Gaussian and Lorentz function. Three quantity are required to define a Gausssian or a Lorentzian band: the eight , the position of the peak, and the bandwidth at half height.

The function B(x) in equation A1.7 allows for the fact that the baseline correction are often necessary and this can be optimized during the curve fitting procedure. More frequently a linear base line of the form

$$Y(x, y_1, y_n) = \frac{y_1 + (x - y_1)(y_n - y_1)}{x_n - x_1}$$

is used, where y_1 is the height of the base line at x_1, and y_n at x_n. The value of the root-mean-square deviation between the calculated and the observed Y values, obtained assuming different band functions, may be used as a guide to the selection of an appropriate function for fit the observed data.

REFERENCES

Auer, L.H., and Mihalas, D., 1972,Ap.J. Suppl. Series 205, 24, 193.

Ando, H.,1976, Publ. Astron. Soc. Japan, 8, 517.

Ando, H., Osaki,Y., 1975, Publ. Astron. soc. Japan, 27, 581.

Baade, D., 1982, Astron. Ap., 105, 65.

Baade, D., 1984, Astron. Ap., 140, 115.

Barker, P.K., 1979, Ph. D. Diss., Univ. Colorado, Boulder.

Bohlin, R.C., 1970, Ap.J., 162, 571.

Burki, G., Maeder, A., and Rufener, F., 1978, Astron. Ap., 65, 363.

Christensen-Dalsgaard, J., and Gough, D.O., 1976, Nature, 259, 89.

Cowley, A.P., Marlborough, J.M., 1968, Publ. Astron. Soc. Pacific, 80, 42.

Cowley, A.P., Rogers, L., Hutchings, J.B., 1976, Publ. Astron. Soc. Pacific, 87, 513.

Cox, J.P., 1980, "Theory of Stellar Pulsation" Princenton University Press.

Doazan, V., Franco, M., Stalio, R., Thomas, R.N., 1982, in " The Be Stars", IAU Symp. 98, eds., Mercedes Jascheck and H.G. Groth, pag. 319.

Doazan, V., Thomas, R. N., 1982 in " The Third IUE European Conference " ESA SP-176, pag. 287.

Doazan, V., Underhill, A., ed.s, 1982,"The B Stars With and Without Emission Lines", NASA SP-456.

Doazan, V., Franco, M., Rusconi, L., Sedmak, G., Stalio, R., 1983, Astron. Ap., 128, 171.

Doazan, V., Franco, M., Rusconi, L., Sedmak, G., Stalio,R.,1984, Astron. Ap. Suppl., 55, 1.

Doazan, V., Thomas, R.N., Barylak, M., 1985, preprint.

Dziembowski, W., 1971, Acta Astron., 21, 289.

Eddington, A.S., 1918, M.N.R.A.S., 79, 177.

Edwards, D.L., 1956, Vistas in Astronomy, 2, 1470.

Frazer, R.D.B., Suzuki, F., 1966, in "Spectral Analysis: Methods and Thechniques", ed. J.A. Blackburn (M. Dekker inc., New York),1970, pag.171.

Huang, S.S., 1977, Ap.J., 212, 123

Hutchings, J.B., 1976, in Proc. IAU Symp. 70, ed. A. Slettebac,k pag. 13.

Jerningan, J.A., 1976, IAU Circ N 2900.

Kitchin, C.R., 1970, Astrophys. Space Sci, 8, 3.

Kubiak, M., 1978, Acta Astron., 28, 153.

Ledoux, P., 1951, Ap.J., 114, 373.

Ledoux, P., Waldraven, Th., 1958, Handbuch der Physik (Springer-Verlag), 51, 353.

Ledoux, P., 1974, in IAU Symp. 59, ed. P. Ledoux, A. Noels, A.W. Rodgers, pag. 135.

Leighton, R.B., Noyes, R.W., Simon, G.W., 1962, Ap.J., 135, 474.

Lucy, L.B., 1976, Ap.J., 206, 499.

Mason, K.O., White, N.E., Stamford, P.W., Hawkins, F.G., Drake, J.F., York, D.G., 1976, M.N.R.S., 176, 193.

Mc Graw, J.T., and Robinson, E.L., 1976, Ap.J. Letters, 205, L155.

Mc Graw, J.T., 1977, Ph. D. Diss., University of Texas.

Maeder, A., Rufener, F., 1981, Workshop on Pulsating B Stars, ed. C. Sterken, Nice Observatory, pag. 65.

Marlborough, J.M., Snow, T.P., Slettebak, K.A., 1978, Ap.J., 224, 157.

Osaki, Y., 1971, Publ. Astr. Soc. Japan, 23, 485.

Pasian, F., Rusconi, L., Sedmak, G., 1982, Elspec/11 Spectrogram Processing, Package. Publ. Oss. Astron. Trieste 806 and 807.

Poeckert, R., Marlborough, J.M., 1978, Ap.J., 220, 940.

Polidan, R.S., Stalio, R., 1985, in *

Rosseland, S.,1949, "The Pulsation Theory of Variable Stars" Oxford:

Claredon Press.

Sculfaire, R., 1974, Astron. Ap., 36, 107.

Shapley, H., 1914, Ap.J., 40, 448.

Slettebak, K.A.,and Snow, T.P., 1978, Ap.J. Letters, 224, L127.

Slettebak, K.A., 1979, Space Sci Rev., 23, 541.

Slettebak, K.A., 1982, Ap.J. Suppl., 50, 55.

Smith, M.A., 1977, Ap.J., 215, 574.

Smith, M.A., Ebbets, D., 1981, Ap.J., 247, 158.

Smith, M.A., 1984, in *

Smith, M.A. and Penrod, G.D., 1985 in *

Struve, O., 1931, Ap.J., 73, 94.

Unno, W., Osaki, Y., Ando, H., Shibahashi, H., "Nonradial Oscillations of Stars" University of Tokio Press, 1979.

Vogt, S.S. Penrod, G.D., 1983, Ap.J., 275, 661.

Walker, G.A.H., Yang, S., Fahalman, G.G., 1979, Ap.J., 233, 199.

* Stalio, R., Zirker, J.B., ed.s ,1985, "Relations between Chromospheric Coronal Heating and Mass Loss in Stars" , Proceedings III-Trieste Workshop, in press.